Bergische Universität Wuppertal

Fachbereich Mathematik und Naturwissenschaften

Lehrstuhl für Angewandte Mathematik
und Numerische Mathematik

Lehrstuhl für Optimierung und Approximation

Preprint BUW-AMNA-OPAP 11/03

Dirk Klindworth, Matthias Ehrhardt and Thomas Koprucki

Discrete Transparent Boundary Conditions for Multiband Effective Mass Approximations

March 2011

http://www.math.uni-wuppertal.de

Discrete Transparent Boundary Conditions for Multiband Effective Mass Approximations

Dirk Klindworth[1], Matthias Ehrhardt[2] and Thomas Koprucki[3]

[1] RWTH Aachen, Lehr- und Forschungsgebiet NLD, Steinbachstr. 15, 52074 Aachen, Germany
[2] Bergische Universität Wuppertal, Fachbereich Mathematik und Naturwissenschaften, Lehrstuhl für Angewandte Mathematik und Numerische Mathematik, Gaußstr. 20, 42119 Wuppertal, Germany
[3] Weierstraß–Institut für Angewandte Analysis und Stochastik, Mohrenstr. 39, 10117 Berlin, Germany

Abstract. This chapter is concerned with the derivation and numerical testing of *discrete transparent boundary conditions* (DTBCs) for stationary *multiband effective mass approximations* (MEMAs). We analyze the continuous problem and introduce *transparent boundary conditions* (TBCs). The discretization of the differential equations is done with the help of finite difference schemes. A fully discrete approach is used in order to develop DTBCs that are completely reflection-free. The analytical and discrete dispersion relations are analyzed in depth and the limitations of the numerical computations are shown. We extend the results of earlier works on DTBCs for the scalar Schrödinger equation by alternative finite difference schemes. The introduced schemes and their corresponding DTBCs are tested numerically on an example with single barrier potential. The d-band $\mathbf{k}\cdot\mathbf{p}$-model is introduced as most general MEMA. We derive DTBCs for the d-band $\mathbf{k}\cdot\mathbf{p}$-model and test our results on a quantum well nanostructure.

1 Introduction

Partial differential equations (PDEs) arise in a wide field of physical problems and often they are posed on unbounded domains. In order to compute a numerical solution to these PDEs one requires a finite computational domain. Usually, this is done by introducing *artificial boundary conditions*. If the solution of the unbounded domain restricted to the computational domain equals the approximate solution when using the artificial boundary conditions, then these boundary conditions are called *transparent boundary conditions* (TBCs).

TBCs of time-dependent Schrödinger equations have been discussed extensively, see for example the review by Antoine et. al. [1]. It has been shown that a fully discrete approach in deriving these TBCs, yielding so-called *discrete transparent boundary conditions* (DTBCs), implies significant numerical advantages. On the other hand, an ad-hoc discretization of the continuous TBCs can result in unphysical reflections at the TBCs and may influence the stability of the numerical scheme [3]. Moreover, this discrete approach was successfully applied to general Schrödinger-type equations [2, 10, 11].

DTBCs for systems of time-dependent Schrödinger equations were developed in [28, 29]. For stationary Schrödinger equations, however, DTBCs have only been developed in the scalar case [4].

The discretization of the differential equations is done using finite differences schemes. For an alternative approach using the finite element method the reader is referred to [22] and the references therein.

In this chapter we will directly consider the general d-band $\mathbf{k}\cdot\mathbf{p}$-model. An analysis of particular MEMAs such as the two-band Kane-model and two-band $\mathbf{k}\cdot\mathbf{p}$-model can be found in [7] and [13].

This chapter is organized as follows: In Section 2 we will summarize the results of the stationary scalar case and extend it to some alternative discretizations. We will compare the dispersion relations of these schemes and their numerical results when applied to a single barrier potential. After that, we will derive DTBCs for the general d-band $\mathbf{k}\cdot\mathbf{p}$-model in Section 3. The DTBCs are tested using a quantum well structure. Finally, we will summarize our work in Section 4 and discuss future research topics.

2 Single-Band Effective Mass Approximations – The Scalar Schrödinger Equation

We start with the stationary linear Schrödinger equation for the wave function $\psi(x)$

$$H\psi = E\psi, \qquad x \in \mathbb{R}, \tag{1}$$

where E denotes the energy of the electron and H is the Hamiltonian operator that reads

$$H = -\frac{\hbar^2}{2m^*}\frac{\mathrm{d}^2}{\mathrm{d}x^2} + V(x), \tag{2}$$

with the reduced Planck constant $\hbar$, the effective mass m^* of the electron and the real-valued potential energy profile $V(x)$ of the electron at the position x.

A solution $\psi_E(x)$ of the stationary linear Schrödinger equation (1) is called an *energy eigenstate* with associated energy E.

We consider a semiconductor of length L connected to reservoirs at $x = 0$ and $x = L$. Let us assume that the potential $V(x)$ is constant in the reservoirs, i.e. we set $V(x) = 0$ if $x \leq 0$ and $V(x) = V_L$ if $x \geq L$. Note that the assumption $V(x) = 0$ for $x \leq 0$ means no loss of generality since we are free to set the energetic zero point. Similarly, the assumption that the left boundary is located at $x = 0$ is no loss of generality.

2.1 The Exterior Problem and the Quantum Mechanical Dispersion Relation

The *exterior problem* is concerned with the solution of the Schrödinger equation in the exterior domains. By assumption, the potential V is constant in these domains and hence,

Eq. (1) becomes a second order ordinary differential equation (ODE) with constant coefficients that reads

$$-\frac{\hbar^2}{2m^*}\frac{\mathrm{d}^2}{\mathrm{d}x^2}\psi = (E-V)\,\psi, \qquad x \in \mathbb{R}. \tag{3}$$

As shown in the basic theory on ODEs the solution of Eq. (3) takes the form

$$\psi(x) = \hat{\psi} e^{\mathrm{i}kx}, \tag{4}$$

where $\hat{\psi} \in \mathbb{C}$ is an arbitrary constant and the complex *wave vector* $k = \hat{k} + \mathrm{i}\check{k}$ is the root of the characteristic polynomial

$$\frac{\hbar^2}{2m^*}k^2 = (E-V)\,.$$

If we assume that the energy satisfies $E > V$, the wave vector k is real and reads

$$k = \pm\hat{k} = \pm\sqrt{\frac{2m^*}{\hbar^2}\,(E-V)}. \tag{5}$$

Note that the resulting waves of the form (4) are traveling. In classical physics the energy condition $E > V$ is always fulfilled since there can only exist particles with an energy greater than the potential at that point. However, in quantum physics this is not the case and therefore, we shall, in general, not require $E > V$ inside the computational domain.

As can be seen from the *quantum mechanical momentum operator* in one dimension, $p = -\mathrm{i}\hbar\frac{\mathrm{d}}{\mathrm{d}x}$, the expectation value of the momentum p of the wave ψ of amplitude 1 is $\langle p\psi, \psi\rangle = \hbar k\,\langle\psi,\psi\rangle = \hbar k$. Hence, the expectation value of the momentum p is proportional to the wave vector k. This means that a positive wave vector corresponds to a positive momentum, i.e. a right-traveling wave, while a negative wave vector corresponds to a negative momentum, i.e. a left-traveling wave.

If the energy does not satisfy the condition $E > V$, the wave vector k is purely imaginary and takes the form

$$k_{1,2} = \pm\mathrm{i}\check{k} = \pm\sqrt{\frac{2m^*}{\hbar^2}\,(V-E)}. \tag{6}$$

This wave vector yields evanescent waves (4).

If we apply the solution (4) to Eq. (3) we obtain

$$\frac{\hbar^2 k^2}{2m^*}\hat{\psi} = (E-V)\,\hat{\psi}.$$

Since we can neglect the trivial solution $\psi \equiv 0$, the energy E satisfies the *quantum mechanical dispersion relation*

$$E = E(k) = V + \frac{\hbar^2 k^2}{2m^*}. \tag{7}$$

2.2 Transparent Boundary Conditions

In order to transform the Schrödinger equation (1) on the real line $x \in \mathbb{R}$ into an equivalent system posed on the bounded domain $(0, L)$ we introduce artificial boundary conditions at $x = 0$ and $x = L$. Artificial boundary conditions that form a system whose solution equals the solution of the unbounded problem on the domain $(0, L)$ are called *transparent boundary conditions* (TBCs).

In order to derive these TBCs we consider a plain wave of amplitude 1 with positive momentum coming from $-\infty$ and entering the computational domain from the left at $x = 0$

$$\psi^{\mathrm{in}} = e^{\mathrm{i}\hat{k}_0 x}, \qquad x < 0, \tag{8}$$

where $\hat{k}_0 > 0$ denotes the propagation coefficient, cf. (5) of the wave vector k in the left exterior domain $x \leq 0$, i.e. with $V \equiv 0$. The incoming wave (8) results in a reflected, left-traveling wave

$$\psi^{\mathrm{r}} = re^{-\mathrm{i}\hat{k}_0 x}, \qquad x < 0, \tag{9a}$$

with the reflection coefficient r, and a transmitted, right-traveling wave

$$\psi^{\mathrm{t}} = te^{\mathrm{i}\hat{k}_L x}, \qquad x > L, \tag{9b}$$

with the transmission coefficient t and the propagation coefficient $\check{k}_L > 0$ of the wave vector k in the right exterior domain $x \geq L$, i.e. with $V \equiv V_L$. The propagation coefficient $\hat{k}_L$ satisfies

$$\hat{k}_L = \sqrt{\hat{k}_0^2 - \frac{2m^* V_L}{\hbar^2}}.$$

Thus, the solution in the left exterior domain has the form

$$\psi = \psi^{\mathrm{in}} + \psi^{\mathrm{r}}, \qquad x < 0, \tag{10a}$$

and the solution in the right exterior domain is

$$\psi = \psi^{\mathrm{t}}, \qquad x > L. \tag{10b}$$

We know that the wave and its first derivative are continuous at the two boundaries, cf. [14]. Hence, we can eliminate the reflection and transmission coefficients by comparing Eq. (10a) and its first derivative at $x = 0$ as well as Eq. (10b) and its first derivative at $x = L$.

The resulting *boundary value problem* (BVP) reads

$$-\frac{\hbar^2}{2m^*}\psi_{xx} + V(x)\psi = E\psi, \qquad 0 < x < L, \tag{11a}$$

$$\psi_x(0) + \mathrm{i}k\psi\,(0) = 2\mathrm{i}\hat{k}_0, \tag{11b}$$

$$\psi_x(L) - \mathrm{i}\sqrt{\hat{k}_0^2 - \frac{2m^* V_L}{\hbar^2}}\psi\,(L) = 0. \tag{11c}$$

Theorem 2.1 (Proposition 2.3 in [6])**.** *Let V be in $L^\infty(0, L)$ and real valued. Then the BVP (11) has a unique solution $\psi \in W^{2,\infty}(0, L)$.*

2.3 The Standard Discretization

After stating the BVP (11) and showing that it has a unique solution, we want to derive techniques to solve it numerically and compute eigenstates for corresponding energies and potentials. First let us set $\hbar = m^* = 1$ for the remainder of this section. We will introduce *finite difference schemes* (FDS) to solve the BVP, using the uniform discretization $x_j = jh,\ j = 0, \ldots, J$ with $L = Jh$, of the computational domain $(0, L)$ and the approximation $f(x_j) \approx f_j$ of some function f defined in $(0, L)$. In the sequel, we will use the following finite difference quotient operators: the first order forward operator $\mathrm{D}_h^{\mathrm{fwd}} f_j := (f_{j+1} - f_j)/h$, the first order backward operator $\mathrm{D}_h^{\mathrm{bwd}} f_j := (f_j - f_{j-1})/h$, the second order centered operator $\mathrm{D}_h^{\mathrm{cen}} f_j := (f_{j+1} - f_{j-1})/2h$ and the standard second order operator $\mathrm{D}_h^{\mathrm{std}} f_j := (f_{j-1} - 2f_j + f_{j+1})/h^2$.

By applying the standard second order finite difference quotient operator we get the *second order standard FDS*

$$-\frac{1}{2}\mathrm{D}_h^{\mathrm{std}}\psi_j + V_j\psi_j = E\psi_j, \qquad j = 1, \ldots, J-1, \tag{12}$$

for the Schrödinger equation (11) with $V_j = V(x_j)$ and the approximation $\psi_j \approx \psi(x_j)$, $j = 0, \ldots, J$. We can rewrite Eq. (12) in the form

$$-\psi_{j+1} + 2\left(1 - (E - V_j)\,h^2\right)\psi_j - \psi_{j-1} = 0, \qquad j = 1, \ldots, J-1. \tag{13}$$

This is a linear second order homogeneous difference equation with a spatially varying coefficient V_j.

Now let us analyze the *discrete exterior problem* of the standard FDS. We will continue with some constant potential V. The results of the exterior domains $x \leq 0$ and $x \geq L$ can later be derived by inserting the respective value of the potential in the results stated.

If V is constant, Eq. (13) is a linear second order difference equation with constant coefficients and as shown in [16], Eq. (13) has a solution of the form

$$\psi_j = \hat{\psi}_h\alpha^j = \hat{\psi}_h e^{\ln(\alpha)j} = \hat{\psi}_h e^{(\ln|\alpha| + \mathrm{i}\arg(\alpha))j} = \hat{\psi}_h e^{\mathrm{i}k_h jh}, \tag{14}$$

with $\alpha \in \mathbb{C}$, cf. (4). We will call $\hat{\psi}_h$ the *discrete amplitude* of the discrete wave ψ_j and

$$k_h = -\mathrm{i}\frac{1}{h}\ln(\alpha) = \frac{1}{h}\left(\arg(\alpha) - \mathrm{i}\ln|\alpha|\right) \tag{15}$$

the *discrete wave vector*. By applying Eq. (14) to Eq. (13) we get

$$-\alpha^{j+1} + 2(1 - (E - V)\,h^2)\alpha^j - \alpha^{j-1} = \alpha^{j-1}\left(\alpha^2 - 2\left(1 - (E - V)\,h^2\right)\alpha + 1\right) = 0.$$

Since we neglect the trivial solution $\alpha = 0$, we have

$$\alpha^2 - 2\left(1 - (E - V)\,h^2\right)\alpha + 1 = 0,$$

which implies

$$\left(\alpha - \left(1 - (E - V)\,h^2\right)\right)^2 = (E - V)\,h^2\left((E - V)\,h^2 - 2\right). \tag{16}$$

If the energy E satisfies $E > V$, the right hand side of Eq. (16) is negative if the step size h satisfies

$$h < \sqrt{\frac{2}{E-V}}, \tag{17}$$

and hence, the roots of Eq. (16) are complex and read

$$\alpha_{1,2} = 1 - (E-V)\,h^2 \pm \mathrm{i}\sqrt{(E-V)\,h^2\,(2-(E-V)\,h^2)}. \tag{18}$$

We find that

$$|\alpha_{1,2}| = \left(1-(E-V)\,h^2\right)^2 + (E-V)\,h^2\left(2-(E-V)\,h^2\right) = 1,$$

and thus, the discrete wave vector k_h is real and takes the form

$$k_h = \pm\hat{k}_h = \pm\frac{1}{h}\arg(\alpha) = \pm\frac{1}{h}\arccos\frac{\operatorname{Re}\alpha}{|\alpha|} = \pm\frac{1}{h}\arccos\left(1-(E-V)\,h^2\right), \tag{19}$$

cf. (5). Note that we can neglect to add the term $n\frac{2\pi}{h}$, $n \in \mathbb{Z}$, to this formula since for any $n \neq 0$ this term diverges for $h \to 0$. On the other hand, we will see later that the discrete wave vector k_h as given in Eq. (19), i.e. with $n = 0$, tends to the analytical wave vector k for $h \to 0$.

The wave vector $k_h = \hat{k}_h$ corresponds to

$$\alpha_1 = 1 - (E-V)\,h^2 + \mathrm{i}\sqrt{(E-V)\,h^2\,(2-(E-V)\,h^2)},$$

while $k_h = -\hat{k}_h$ is associated with

$$\alpha_2 = 1 - (E-V)\,h^2 - \mathrm{i}\sqrt{(E-V)\,h^2\,(2-(E-V)\,h^2)}.$$

Hence, we get two traveling waves, $\psi_j = \alpha_1^j$ being right-traveling and $\psi_j = \alpha_2^j$ being left-traveling.

The case

$$h \geq \sqrt{\frac{2}{E-V}},$$

results in a non-negative right hand side of Eq. (16) and thus, a complex conjugate pair of purely imaginary wave vectors that give evanescent waves. However, this case is numerically not applicable since it defines a lower bound for the step size h.

On the other hand, if $E \leq V$, the right hand side of Eq. (16) is also non-negative, yielding a complex conjugate pair of purely imaginary wave vectors that give evanescent waves. Let us recall the TBCs we derived in Section 2.2. We considered an incoming wave, i.e. a traveling wave to enter the semiconductor at $x = 0$. Hence, the case $E \leq V$ is not applicable either for the exterior domains since it leads to evanescent waves only.

Now let us analyze the behavior of the discrete wave vector k_h of the standard FDS for $h \to 0$. To this end, we apply l'Hôpital's rule to get

$$\begin{aligned}\lim_{h\to 0} k_h &= \pm \lim_{h\to 0} \hat{k}_h = \pm \lim_{h\to 0} \frac{1}{h} \arccos\left(1 - (E-V)\, h^2\right) \\ &= \pm \lim_{h\to 0} \frac{-2\,(E-V)\, h}{\sqrt{1-\left(1-(E-V)\, h^2\right)^2}} = \pm\sqrt{2\,(E-V)},\end{aligned}$$

which equals the analytical wave vector (5) for $\hbar = m^* = 1$.

Note, that Eq. (19) defines the *discrete dispersion relation*. Finally, we will state this relation in the reciprocal form. Recall the wave representation of the form $\psi_j = \hat{\psi} e^{\mathrm{i} k_h j h}$ that implies $\psi_{j+1} e^{-\mathrm{i}kh} = \psi_j = \psi_{j-1} e^{\mathrm{i}kh}$. Applied to the difference equation (13), this gives

$$-e^{\mathrm{i}kh} + 2\left(1 - (E-V)\, h^2\right) - e^{-\mathrm{i}kh} = 0,$$

which leads to

$$E = E_h^{\mathrm{std}}(k_h) = V + \frac{1-\cos k_h h}{h^2} = V + \frac{2}{h^2}\sin^2\frac{k_h h}{2} = V + \frac{k_h^2 h}{2} + \mathcal{O}(h^2), \tag{20}$$

compared to the continuous dispersion relation (7).

2.4 Discretization of the Transparent Boundary Conditions

Let us now introduce a finite difference discretization of the two Robin-type TBCs (11b) and (11c). We apply the second order centered difference operator $\mathrm{D}_h^{\mathrm{cen}}$ to ψ_0 at the left boundary and ψ_J at the right boundary. Let $\hat{k}_0$ denote the analytical propagation coefficient of a right-traveling wave in the left exterior domain $x \le 0$. Then the analytical propagation coefficient of a right-traveling wave in the right exterior domain is

$$\hat{k}_L = \sqrt{\hat{k}_0^2 - 2V_L}.$$

At the left boundary we have

$$\frac{\psi_1 - \psi_{-1}}{2h} + \mathrm{i}\hat{k}_0 \psi_0 = 2\mathrm{i}\hat{k}_0,$$

which implies

$$-\psi_{-1} + 2\mathrm{i}\hat{k}_0 h \psi_0 + \psi_1 = 4\mathrm{i}\hat{k}_0 h. \tag{21a}$$

On the other hand, discretizing the right TBC gives

$$\frac{\psi_{J+1} - \psi_{J-1}}{2h} = \mathrm{i}\sqrt{\hat{k}_0^2 - 2V_L}\,\psi_J,$$

that can be expressed in the form

$$\psi_{J-1} + 2\mathrm{i}\sqrt{\hat{k}_0^2 - 2V_L}\, h \psi_J - \psi_{J+1} = 0. \tag{21b}$$

The two ghost points ψ_{-1} and ψ_{J+1} in Eq. (21) can be eliminated by subtracting the FDS (13) of the Schrödinger equation (11a) at $j = 0$ and $j = J$. By using the identities $E = \hat{k}_0^2/2$ and $E - V_L = \hat{k}_L^2/2$ we get the two second order discretized TBCs

$$\left(\frac{1}{2}\hat{k}_0^2 h^2 - 1 + \mathrm{i}\hat{k}_0 h\right)\psi_0 + \psi_1 = 2\mathrm{i}\hat{k}_0 h \tag{22a}$$

and

$$\psi_{J-1} + \left(\frac{1}{2}\left(\hat{k}_0^2 - 2V_L\right)h^2 - 1 + \mathrm{i}\sqrt{\hat{k}_0^2 - 2V_L}\,h\right)\psi_J = 0. \tag{22b}$$

Existence and uniqueness of the solution of the numerical scheme together with the discretized TBCs is shown in

Theorem 2.2 (Theorem 2.1 in [4]). *Let* $\{V_j\}, j = 0, \ldots, J$, *and* $E > \max\{0, V_L\}$ *be given, and assume* $h < \min\left\{\sqrt{\frac{2}{E}}, \sqrt{\frac{2}{E-V_L}}\right\}$. *Then the discrete BVP (13) with the discretized TBCs (22) has a unique solution* $\{\psi_j\}, j = 0, \ldots, J$.

Let us recall the discrete waves $\psi_j = e^{\mathrm{i}\hat{k}_{h,0}jh}$ in the left exterior domain $j \leq 0$ and $\psi_j = e^{\mathrm{i}\hat{k}_{h,L}jh}$ in the right exterior domain $j \geq J$. Suppose that they are solutions to the difference scheme in a small vicinity of the two boundaries, i.e. $j = 0, 1$ and $j = J-1, J$. Then they should also satisfy the discretized TBCs (22). However, at the left boundary we get

$$\begin{aligned}
2\mathrm{i}\hat{k}_0 h &= \left(Eh^2 - 1 + \mathrm{i}\hat{k}_0 h\right)\psi_0 + \psi_1 = \left(Eh^2 - 1 + \mathrm{i}\hat{k}_0 h\right) + e^{\mathrm{i}\hat{k}_{h,0}h} \\
&= \left(Eh^2 - 1 + \mathrm{i}\hat{k}_0 h\right) + \left(1 - Eh^2 + \mathrm{i}\sqrt{2Eh^2 - E^2h^4}\right) \\
&= \mathrm{i}\hat{k}_0 h + \mathrm{i}\hat{k}_0 h\sqrt{1 - \hat{k}_0^2 h^2/4} \neq 2\mathrm{i}\hat{k}_0 h,
\end{aligned}$$

which is a contradiction. A similar contradiction can be found at the right boundary.

The reason is that the TBCs are based on the analytical solution as derived in Section 2.1. The wave vector of the analytical solution, see Eq. (5), however, is different from the discrete wave vector (19). Hence, the discretized TBCs model exterior domains whose physical properties (i.e. wave vector and dispersion relation) are discretization of the analytical properties. Inside the computational domain, however, we use the FDS (13) that implies a discrete wave vector and a discrete dispersion relation. In other words, a wave coming from $-\infty$ and entering the semiconductor at $x = 0$ is *refracted* at the boundary $x = 0$ as it comes from a media with the analytical dispersion relation and enters a media with the discrete dispersion relation. This leads to spurious oscillations in the numerical solution.

2.5 Discrete Transparent Boundary Conditions

In this section we will derive the *discrete transparent boundary conditions* (DTBCs) of the single-band model. DTBCs are derived on a fully discrete level. This means that they are

deduced with the help the discrete exterior solution as given in Eq. (14). We assume that the discrete exterior solution holds in a small vicinity of the two boundaries. Consequently, the refraction at the boundaries, resulting in spurious oscillations, vanishes completely.

Let us recall the right-traveling discrete wave $\psi_j = e^{\mathrm{i}\hat{k}_h jh}$ and the left-traveling discrete wave $\psi_j = e^{-\mathrm{i}\hat{k}_h jh}$ with discrete amplitude $\hat{\psi}_h = 1$. Let $\hat{k}_{h,0}$ denote the discrete wave vector in the left exterior domain $x \leq 0$, i.e. with $V \equiv 0$, and $\hat{k}_{h,L}$ the discrete wave vector in the right exterior domain $x \geq L$, i.e. with $V \equiv V_L$. We apply these discrete waves to the reflection and transmission conditions (10) and consider that they hold in a small vicinity of the two boundaries, i.e. $j = 0, 1$ and $j = J-1, J$ respectively. It yields

$$\psi_j = \psi_j^{\mathrm{in}} + \psi_j^{\mathrm{r}} = e^{\mathrm{i}\hat{k}_{h,0}x_j} + re^{-\mathrm{i}\hat{k}_{h,0}x_j}, \qquad j = 0, 1,$$

and

$$\psi_j = \psi_j^{\mathrm{t}} = te^{\mathrm{i}\hat{k}_{h,L}x_j}, \qquad j = J-1, J.$$

By eliminating the reflection and transmission coefficients we obtain the DTBCs

$$-\psi_0 e^{-\mathrm{i}\hat{k}_{h,0}h} + \psi_1 = 2\mathrm{i}\sin\hat{k}_{h,0}h, \tag{23a}$$

and

$$\psi_{J-1}e^{\mathrm{i}\hat{k}_{h,L}h} - \psi_J = 0, \tag{23b}$$

cf. the TBCs (11b) and (11c).

Let us recall the discretized TBCs (22). We expand the exponential function and the sine function in the left DTBC (23a). Keeping terms up to second order gives

$$-\left(1 - \mathrm{i}\hat{k}_{h,0}h - \frac{1}{2}\hat{k}_{h,0}^2h^2\right)\psi_0 + \psi_1 = 2\mathrm{i}\hat{k}_{h,0}h.$$

If we replace the discrete wave vector $\hat{k}_{h,0}$ by the analytical wave vector $\hat{k}_0$ the above equation becomes

$$\left(\frac{1}{2}\hat{k}_0^2h^2 - 1 + \mathrm{i}\hat{k}_0h\right)\psi_0 + \psi_1 = 2\mathrm{i}\hat{k}_0h,$$

which equals the left discretized TBC. Similarly, we can deduce the right discretized TBC from the right DTBC.

Now we can reformulate Theorem 2.2 for the DTBCs.

Theorem 2.3 (Theorem 2.1 in [4]). *Let $\{V_j\}, j = 0, \ldots, J$, and $E > \max\{0, V_L\}$ be given, and assume $h < \min\left\{\sqrt{\frac{2}{E}}, \sqrt{\frac{2}{E-V_L}}, \frac{\pi}{\hat{k}_{h,0}}, \frac{\pi}{\hat{k}_{h,L}}\right\}$. Then the discrete BVP (13) with the DTBCs (23) has a unique solution $\{\psi_j\}, j = 0, \ldots, J$.*

2.6 Alternative Finite Difference Schemes

In this section we derive and compare alternative FDSs. Our aim is to improve the convergence of the scheme or to develop schemes that solve the problem exactly if certain conditions are fulfilled.

2.6.1 The Numerov Discretization

We start with the so-called *Numerov discretization* [21] that is of higher order than the standard discretization.

Let us consider the Schrödinger equation of the BVP (11), and let us rewrite it in the form

$$\psi_{xx} = -2\left(E - V\left(x\right)\right)\psi, \qquad 0 < x < L. \tag{24}$$

As before, we use the uniform grid $x_j = jh,\ j = 0, \ldots, J$ with $L = Jh$. From Eq. (24) together with the standard second order finite difference operator $\mathrm{D}_h^{\mathrm{std}}$ we find that

$$\begin{aligned} h^2\psi_j^{(iv)} &= h^2 \left.\frac{\mathrm{d}^2}{\mathrm{d}x^2}\psi_{xx}\left(x\right)\right|_{x=x_j} \\ &= h^2\left(-2\left.\frac{\mathrm{d}^2}{\mathrm{d}x^2}\left(\left(E - V\left(x\right)\right)\psi\right)\right|_{x=x_j}\right) \\ &= h^2\left(-2\mathrm{D}_h^{\mathrm{std}}\left(\left(E - V_j\right)\psi_j\right) + \mathcal{O}\left(h^2\right)\right) \\ &= -2\left(E - V_{j+1}\right)\psi_{j+1} + 4\left(E - V_j\right)\psi_j - 2\left(E - V_{j-1}\right)\psi_{j-1} + \mathcal{O}\left(h^4\right). \end{aligned} \tag{25}$$

On the other hand, the Taylor series

$$\psi(x \pm h) = \psi(x) \pm h\psi_x(x) + \frac{h^2}{2}\psi_{xx}(x) \pm \frac{h^3}{6}\psi_{xxx}(x) + \frac{h^4}{24}\psi^{(iv)}(x) \pm \frac{h^5}{96}\psi^{(v)}(x) + \mathcal{O}(h^6)$$

gives

$$\psi(x+h) + \psi(x-h) = 2\psi(x) + h^2\psi_{xx}(x) + \frac{h^4}{12}\psi^{(iv)}(x) + \mathcal{O}(h^6),$$

which implies

$$h^2\psi_j^{(iv)} = \frac{12}{h^2}\left(\psi_{j+1} - 2\psi_j + \psi_{j-1}\right) - 12\ \psi_{xx}(x)|_{x=x_j} + \mathcal{O}(h^4).$$

If we apply Eq. (24) to the above equation we get

$$h^2\psi_j^{(iv)} = \frac{12}{h^2}\left(\psi_{j+1} - 2\left(1 - \left(E - V_j\right)h^2\right)\psi_j + \psi_{j-1}\right) + \mathcal{O}(h^4). \tag{26}$$

A comparison of Eqs. (25) and (26) gives the Numerov FDS

$$\begin{aligned} \left(1 + \frac{h^2}{6}\left(E - V_{j+1}\right)\right)\psi_{j+1} - 2\left(1 - \frac{5h^2}{6}\left(E - V_j\right)\right)\psi_j \\ + \left(1 + \frac{h^2}{6}\left(E - V_{j-1}\right)\right)\psi_{j-1} = 0, \qquad j = 1, \ldots, J-1. \end{aligned} \tag{27}$$

The Numerov FDS is of of fourth order if $\psi \in C^6(0, L)$ compared to second order accuracy of the standard FDS if $\psi \in C^4(0, L)$.

Now we will examine the discrete exterior problem of the Numerov FDS with V constant. We want to determine a solution of the discrete exterior problem in order to apply the DTBCs (23).

If V is constant Eq. (27) is a linear second order difference equation with constant coefficients whose solution takes the form

$$\psi_j = \hat{\psi}_h \alpha^j = \hat{\psi}_h e^{\mathrm{i}k_h jh}, \tag{28}$$

with $\alpha \in \mathbb{C}$. Again we will refer to $\hat{\psi}_h$ as the *discrete amplitude* of the discrete wave ψ_j and

$$k_h = -\mathrm{i}\frac{1}{h}\ln(\alpha) = \frac{1}{h}\left(\arg(\alpha) - \mathrm{i}\ln|\alpha|\right) \tag{29}$$

as the *discrete wave vector*. Analogously to the standard FDS we get the discrete solution α by applying Eq. (28) to Eq. (27). Under the assumption that $E > V$ and the step size h satisfies

$$h < \frac{3}{\sqrt{E-V}}, \tag{30}$$

α is complex and reads

$$\alpha_{1,2} = 1 - \frac{6(E-V)h^2}{6+(E-V)h^2} \pm \mathrm{i}\frac{\sqrt{24(E-V)h^2\left(3-(E-V)h^2\right)}}{6+(E-V)h^2}. \tag{31}$$

The modulus of α is

$$|\alpha_{1,2}| = \left(1 - \frac{6(E-V)h^2}{6+(E-V)h^2}\right)^2 + \frac{24(E-V)h^2\left(3-(E-V)h^2\right)}{\left(6+(E-V)h^2\right)^2} = 1.$$

Thus, the discrete wave vector k_h is real and takes the form

$$k_h = \pm\hat{k}_h = \pm\frac{1}{h}\arg(\alpha) = \pm\frac{1}{h}\arccos\frac{\mathrm{Re}\,\alpha}{|\alpha|} = \pm\frac{1}{h}\arccos\left(1 - \frac{6(E-V)h^2}{6+(E-V)h^2}\right), \tag{32}$$

Again we can neglect to add the term $n\frac{2\pi}{h}$, $n \in \mathbb{Z}$, to this formula since for any $n \neq 0$ this term diverges for $h \to 0$. On the other hand, it is easy to show that the discrete wave vector k_h as given in Eq. (32), i.e. with $n = 0$, tends to the analytical wave vector k as given in Eq. (5) for $h \to 0$ and $\hbar = m^* = 1$.

Hence, we get two traveling waves, the right-traveling wave $\psi_j = \alpha_1^j = e^{\mathrm{i}\hat{k}_h jh}$ and the left-traveling wave $\psi_j = \alpha_2^j = e^{-\mathrm{i}\hat{k}_h jh}$.

On the other hand, if the step size h does not satisfy the step size restriction (30) or the energy E does not satisfy the energy condition $E > V$, α is real and yields evanescent waves.

Finally, we derive the *discrete dispersion relation* of the Numerov FDS in the same way as for the standard FDS. The wave $\psi_j = \hat{\psi}e^{\mathrm{i}k_h jh}$ implies $\psi_{j+1}e^{-\mathrm{i}k_h h} = \psi_j = \psi_{j-1}e^{\mathrm{i}k_h h}$, and hence, applied to the Numerov difference equation (27) we get

$$E = E_h^{\mathrm{Num}}(k) = \frac{6}{5+\cos k_h h}\frac{2}{h^2}\sin^2\frac{k_h h}{2}. \tag{33}$$

Now we will prove an analogon to Theorem 2.3.

Theorem 2.4. *Let* $\{V_j\}, j = 0, \ldots, J$, *and* $E > \max\{0, V_L\}$ *be given, and suppose*

$$h < \min\left\{\sqrt{\frac{3}{E}}, \sqrt{\frac{3}{E-V_L}}, \sqrt{\frac{6}{|E-V_1|}}, \sqrt{\frac{6}{|E-V_{J-1}|}}, \frac{\pi}{\hat{k}_{h,0}}, \frac{\pi}{\hat{k}_{h,L}}\right\}.$$

Then the discrete BVP (27) of the Numerov FDS with the DTBCs (23) has a unique solution $\{\psi_j\}, j = 0, \ldots, J$.

Proof. We show that for homogeneous DTBCs the discrete solution is zero at every grid point. Therefore, let us introduce $\varphi_j = \sigma_j \psi_j$ with $\sigma_j = 1 + \frac{h^2}{6}(E - V_j) \in \mathbb{R}$. Note that $\sigma_j > 0$ for $j = 0, 1, J-1, J$.

Now we can rewrite the Numerov FDS in the form

$$\varphi_{j+1} - 2\varphi_j + \varphi_{j-1} = -2h^2 (E - V_j)\psi_j = -2h^2 (E - V_j)\sigma_j^{-1}\varphi_j,$$

or

$$\mathrm{D}_h^{\mathrm{std}}\varphi_j = -2(E - V_j)\sigma_j^{-1}\varphi_j.$$

The homogeneous left DTBC can be written in the form

$$-\gamma_1\psi_0 + \psi_1 = -\gamma_1\sigma_0^{-1}\varphi_0 + \sigma_1^{-1}\varphi_1,$$

that reduces to

$$\mathrm{D}_h^{\mathrm{bwd}}\varphi_1 = \left(\gamma_1\sigma_1\sigma_0^{-1} - 1\right)\varphi_0,$$

with $\gamma_1 = e^{-\mathrm{i}\hat{k}_{h,0}h}$. On the other hand, the right DTBC is

$$\psi_{J-1} - \gamma_2\psi_J = \sigma_{J-1}^{-1}\varphi_{J-1} - \gamma_2\sigma_J^{-1}\varphi_J,$$

which becomes

$$\mathrm{D}_h^{\mathrm{bwd}}\varphi_J = \left(\gamma_2^{-1}\sigma_J\sigma_{J-1}^{-1} - 1\right)\varphi_{J-1},$$

with $\gamma_2 = e^{-\mathrm{i}\hat{k}_{h,L}h}$.

We multiply the sum of the Numerov FDS for $j = 1, \ldots, J-1$ by $\bar{\varphi}_j$, apply the discrete analogon of the integration by parts rule and take the imaginary part to get

$$0 = -\sigma_1\sigma_0^{-1}\operatorname{Im}\gamma_1 |\varphi_0|^2 + \sigma_J\sigma_{J-1}^{-1}\operatorname{Im}\gamma_2^{-1} |\varphi_{J-1}|^2,$$

with

$$\operatorname{Im}\gamma_1 = -\sin\hat{k}_{h,0}h < 0, \qquad h < \frac{\pi}{\hat{k}_{h,0}},$$

and

$$\operatorname{Im}\gamma_2^{-1} = -\frac{1}{|\gamma_2|^2}\operatorname{Im}\gamma_2 = \sin\hat{k}_{h,0}h > 0, \qquad h < \frac{\pi}{\hat{k}_{h,L}}.$$

Hence, we end up with the equation

$$0 = \sigma_1 \sigma_0^{-1} \sin \hat{k}_{h,0} h \left|\varphi_0\right|^2 + \sigma_J \sigma_{J-1} \sin \hat{k}_{h,L} h \left|\varphi_{J-1}\right|^2 .$$

Since $\sigma_j > 0$ for $j = 0, 1, J-1, J$, the above equation implies $\left|\varphi_0\right|^2 = \left|\varphi_{J-1}\right|^2 = 0$. Thus, $\psi_0 = \psi_{J-1} = 0$ and by using the homogeneous DTBCs we get $\psi_1 = 0$ and $\psi_J = 0$. Successively applying the Numerov FDS gives $\psi_j = 0$ for $j = 0, \ldots, J$ and hence, the discrete solution vanishes at every grid point if the DTBCs are homogeneous. Thus, the coefficient matrix of the system of linear equations formed by the discrete BVP and the two DTBCs is regular. This implies that the discrete solution is unique. □

2.6.2 The Mickens Discretization

We recall the Schrödinger equation (1)

$$\psi_{xx} + 2\left(E - V\left(x\right)\right)\psi = 0, \qquad 0 < x < L. \tag{34}$$

Let us assume that the potential $V\left(x\right) \equiv V$ is constant. As shown in Section 2.1 the Schrödinger equation (34) yields a traveling wave if $E > V$ and an evanescent wave otherwise. Hence, in the case $2\left(E - V\right) \equiv c_1 > 0$, Eq. (34) has the solution

$$\psi\left(x\right) = a_1 \cos\left(\sqrt{c_1} x\right) + b_1 \sin\left(\sqrt{c_1} x\right), \tag{35a}$$

and if $2\left(E - V\right) \equiv -c_2 < 0$, Eq. (34) has the solution

$$\psi\left(x\right) = a_2 \cosh\left(\sqrt{c_2} x\right) + b_2 \sinh\left(\sqrt{c_2} x\right), \tag{35b}$$

where $a_1, a_2, b_1, b_2 \in \mathbb{C}$ are arbitrary constants. The *Mickens nonstandard finite difference discretization*

$$\psi_{j+1} - 2\cos\left(h\sqrt{c_1}\right)\psi_j + \psi_{j-1} = 0, \qquad j = 1, \ldots, J-1, \tag{36a}$$

if $E > V$, and

$$\psi_{j+1} - 2\cosh\left(h\sqrt{c_2}\right)\psi_j + \psi_{j-1} = 0, \qquad j = 1, \ldots, J-1, \tag{36b}$$

if $E \leq V$, is a so-called *exact FDS* of Eq. (34) with the solutions (35), cf. [17]. An FDS is said to be *exact* if the numerical solution equals the analytical solution at the grid points, see [15]. It is easy to see that if V is constant the difference equation (36a) has the solution (35a) whereas the difference equation (36b) has the solution (35b). Therefore, the Mickens FDS gives a numerical solution that is equal to the analytical solution at the grid points, in other words, the Mickens FDS is exact.

Now we allow the potential $V(x)$ to vary inside the computational domain $(0, L)$. The Mickens FDS (36) becomes

$$\psi_{j+1} - 2D_j\psi_j + \psi_{j-1} = 0, \qquad j = 1, \ldots, J-1, \tag{37}$$

with

$$D_j = \begin{cases} \cos\left(h\sqrt{2\left(E-V_j\right)}\right), & E > V_j, \\ \cosh\left(h\sqrt{2\left(V_j-E\right)}\right), & E \leq V_j. \end{cases}$$

While the Mickens FDS (37) is exact for a constant potential V it is formally of order $\mathcal{O}(h^2)$ if the potential V is not constant, cf. [9].

In order to use the DTBCs for the Mickens FDS (37) we have to determine a discrete solution of the Mickens FDS in the exterior domains. The Mickens FDS is exact in the exterior domains since the potential V is assumed to be constant in these domains. Hence, the discrete solution is given by the analytical solution as derived in Section 2.1. The discrete wave vector k_h of the Mickens FDS is equal to the analytical wave vector k as given in Eq. (5), and the discrete dispersion relation $E_h^{\mathrm{Mic}}(\hat{k})$ is equal to the analytical dispersion relation (7).

Theorem 2.5. *Let $\{V_j\}, j = 0, \ldots, J$, and $E > \max\{0, V_L\}$ be given, and assume $h < \min\left\{\frac{\pi}{\hat{k}_{h,0}}, \frac{\pi}{\hat{k}_{h,L}}\right\}$. Then the discrete BVP (36) of the Mickens FDS with the DTBCs (23) has a unique solution $\{\psi_j\}, j = 0, \ldots, J$.*

Proof. Let us rewrite the Mickens FDS in the form

$$\mathrm{D}_h^{\mathrm{std}}\psi_j = -\frac{2}{h^2}\left(1 - D_j\right)\psi_j.$$

Since $-\frac{2}{h^2}\left(1 - D_j\right) \in \mathbb{R}$ for all $j = 1, \ldots, J-1$, it becomes clear that this theorem is a direct corollary of Theorem 2.3 and hence, the solution is unique. □

2.6.3 The Numerov-Mickens Discretization

Chen et al. [9] combined the Numerov discretization with the Mickens discretization and proposed the so-called *combined Numerov-Mickens finite-difference scheme*

$$\left(1 + \frac{h^2}{6}\left(E - V_{j+1}\right)\right)\psi_{j+1} - 2D_j\psi_j + \left(1 + \frac{h^2}{6}\left(E - V_{j-1}\right)\right)\psi_{j-1} = 0, \tag{38}$$

for $j = 1, \ldots, J-1$, with

$$D_j = \begin{cases} \cos\left(h\sqrt{2\left(E-V_j\right)}\right), & E > V_j, \\ \cosh\left(h\sqrt{2\left(V_j-E\right)}\right), & E \leq V_j. \end{cases}$$

It can be shown that the Numerov-Mickens FDS (38) is of order $\mathcal{O}\left(h^4\right)$, just as the Numerov FDS, and that it is an exact FDS if the potential V is constant, just as the Mickens FDS, cf. [9].

Let us now study the discrete exterior problem of the Numerov-Mickens FDS with a constant potential V. If V is constant Eq. (38) is a linear second order difference equation with constant coefficients whose solution takes the form

$$\psi_j = \hat{\psi}_h \alpha^j = \hat{\psi}_h e^{\mathrm{i}k_h jh}, \tag{39}$$

with $\alpha \in \mathbb{C}$, the *discrete amplitude* ψ_j and the *discrete wave vector*

$$k_h = -\mathrm{i}\frac{1}{h}\ln(\alpha) = \frac{1}{h}\left(\arg(\alpha) - \mathrm{i}\ln|\alpha|\right). \tag{40}$$

By applying Eq. (39) to Eq. (38) and under the assumption that the energy E satisfies $E > V$, α is complex and reads

$$\alpha_{1,2} = \frac{\cos\left(h\sqrt{2(E-V)}\right)}{1 + h^2(E-V)/6} \pm \mathrm{i}\sqrt{1 - \frac{\cos^2\left(h\sqrt{2(E-V)}\right)}{\left(1 + h^2(E-V)/6\right)^2}}. \tag{41}$$

Note that the step size h has to satisfy

$$\cos^2\left(h\sqrt{2(E-V)}\right) < \left(1 + h^2(E-V)/6\right)^2. \tag{42}$$

But this condition is fulfilled for any step size $h > 0$ since the left hand side of Eq. (42) is in $[0, 1]$, while the right hand side is always greater than 1. It is easy to show that $|\alpha| = 1$ and hence, the discrete wave vector k_h of the Numerov-Mickens FDS is real and reads

$$k_h = \pm\hat{k}_h = \pm\frac{1}{h}\arg(\alpha) = \pm\frac{1}{h}\arccos\frac{\mathrm{Re}\,\alpha}{|\alpha|} = \pm\frac{1}{h}\arccos\frac{\cos\left(h\sqrt{2(E-V)}\right)}{1 + h^2(E-V)/6}. \tag{43}$$

Again we shall neglect to add the term $n\frac{2\pi}{h}$, $n \in \mathbb{Z}$, to this formula since for any $n \neq 0$ this term diverges for $h \to 0$. However, the limit for $h \to 0$ of the discrete wave vector k_h as given in Eq. (43), i.e. with $n = 0$, is undefined. In fact, the discrete wave vector k_h does not converge to the analytical wave vector k and hence, the Numerov-Mickens FDS does not converge for $h \to 0$. Nevertheless, we will continue to analyze this FDS and formulate DTBCs with the right-traveling wave $\psi_j = \alpha_1^j = e^{\mathrm{i}\hat{k}jh}$ and the left-traveling wave $\psi_j = \alpha_2^j = e^{-\mathrm{i}\hat{k}jh}$.

An explicit formula of the *discrete dispersion relation* of the Numerov-Mickens FDS cannot be derived. However, the discrete wave $\psi_j = \hat{\psi}e^{\mathrm{i}k_h jh}$ implies $\psi_{j+1}e^{-\mathrm{i}kh} = \psi_j = \psi_{j-1}e^{\mathrm{i}kh}$. Applied to the difference equation (38) we get

$$\cos\left(h\sqrt{2\left(E_h^{\mathrm{NumMic}} - v\right)}\right) - \left(\frac{h^2}{6}\cos kh\right)\left(E_h^{\mathrm{NumMic}} - V\right) - \cos kh = 0. \tag{44}$$

By numerically evaluating Eq. (44) for $h = 1/100$ and $V = 0$ with the MATLAB procedure `fsolve` using the tolerance 10^{-9}, we obtain the discrete dispersion relation E_h^{NumMic} as shown in Fig. 1.

Although the bad numerical behavior has been illustrated we shall prove

Theorem 2.6. *Let* $\{V_j\}, j = 0, \ldots, J$, *and* $E > \max\{0, V_L\}$ *be given, and assume*

$$h < \min\left\{\sqrt{\frac{6}{|E - V_1|}}, \sqrt{\frac{6}{|E - V_{J-1}|}}, \frac{\pi}{\hat{k}_{h,0}}, \frac{\pi}{\hat{k}_{h,L}}\right\}.$$

Then the discrete BVP (38) of the combined Numerov-Mickens FDS with the DTBCs (23) has a unique solution $\{\psi_j\}, j = 0, \ldots, J$.

Proof. Let us introduce $\varphi_j = \sigma_j \psi_j$ with $\sigma_j = 1 + \frac{h^2}{6}(E - V_j) \in \mathbb{R}$. Note that $\sigma_j > 0$ for $j = 0, 1, J-1, J$.

We rewrite the Numerov-Mickens FDS in the form

$$\mathrm{D}_h^{\mathrm{std}} \varphi_j = -\frac{2}{h^2}\left(1 - \sigma_j^{-1} D_j\right)\varphi_j.$$

Since $-\frac{2}{h^2}\left(1 - \sigma_j^{-1} D_j\right) \in \mathbb{R}$ for all $j = 1, \ldots, J-1$, it becomes clear that this theorem is a direct corollary of Theorem 2.4 and hence, the solution is unique. □

2.6.4 Comparison of the Discrete Dispersion Relations

In the previous sections we introduced FDSs for the BVP (11) and derived the corresponding discrete dispersion relations. Now we want to compare these discrete dispersion relations with the analytical quantum mechanical dispersion relation (7). Fig. 1 shows the analytical and discrete dispersion relations for a step size $h = 1/100$ and a potential $V = 0$.

All discrete dispersion relations except the dispersion relation of the Mickens FDS are periodic in the wave vector k_h with the period $\frac{2\pi}{h} \approx 628$. We can see that for small values of the wave vector, i.e. $k_h < 100$, the dispersion relation of the Numerov FDS coincides with the analytical dispersion relation for the used level of detail in Fig. 1, while the dispersion relation of the combined Numerov-Mickens FDS differs significantly from the analytical dispersion relation. Particularly, for $E = 500$, the value of the energy we used in our examples, the error of the dispersion relation of the Numerov-Mickens FDS is greater than of the other FDSs. This explains the significantly greater phase error of the Numerov-Mickens FDS we observed in Section 2.6.3.

2.7 Numerical Example – The Single Barrier Potential

In this section we analyze the results of the four introduced FDSs in the case of a single barrier potential. We consider a semiconductor of length L composed of two different materials, e.g. GaAs (gallium arsenide) and AlGaAs (aluminium gallium arsenide), where the latter is built between two parts of the first material. Let $0 < x_1 < x_2 < L$ and let the domain $[x_1, x_2)$ be composed of AlGaAs, while the two outer domains $[0, x_1)$ and $[x_2, L]$ are composed of GaAs. $V(x) = E_{\mathrm{c}}(x)$ describes the band edge profile or the variation of the conduction band edge of the semiconductor materials. We call $V_0 = \Delta E_{\mathrm{c}} =$

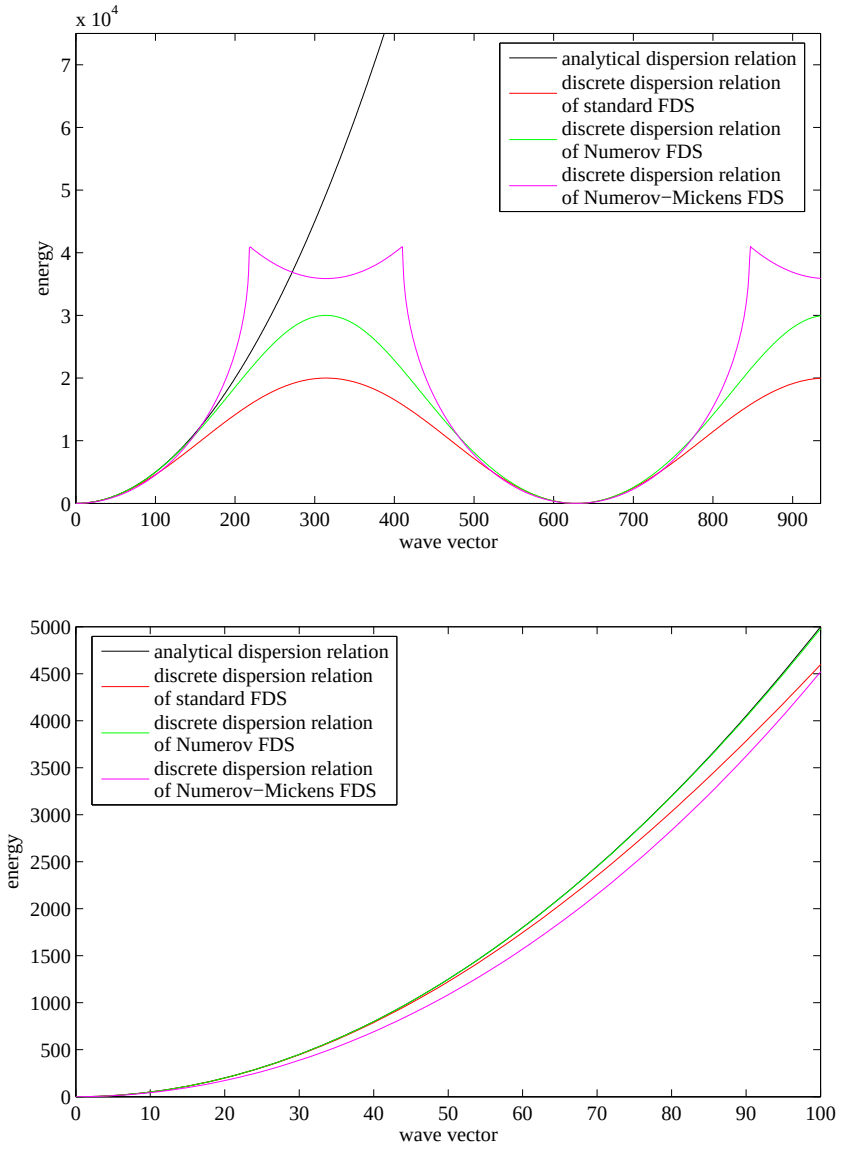

Figure 1: Analytical quantum mechanical dispersion relation $E(k)$ (black), the discrete dispersion relation of the standard discretization $E_h^{\mathrm{std}}(k_h)$ (red), the discrete dispersion relation of the Numerov discretization $E_h^{\mathrm{Num}}(k_h)$ (green) and the discrete dispersion relation of the combined Numerov-Mickens discretization $E_h^{\mathrm{NumMic}}(k_h)$ (magenta) for the step size $h = 1/100$. Note that the discrete dispersion relation of the Mickens discretization $E_h^{\mathrm{Mic}}(k_h)$ coincides with the analytical quantum mechanical dispersion relation $E(k)$.

$E_c|_{\text{AlGaAs}} - E_c|_{\text{GaAs}}$ *band edge offset* between the semiconductor materials or band edge discontinuity of the material interface. The inner domain $[x_1, x_2)$ is called *quantum barrier* if its potential $V(x) = E_c|_{\text{AlGaAs}}$ is greater than the potential $V(x) = E_c|_{\text{GaAs}}$ of the outer domains and *quantum well* if it is smaller.

For simplicity we set $E_c|_{\text{GaAs}} = 0$ and we assume that $E_c|_{\text{AlGaAs}} = 500$, i.e. the band edge offset is $V_0 = \Delta E_c = 500$ and we have a quantum barrier at $x_1 \leq x < x_2$. Furthermore, we set $L = 1$, $x_1 = 1/3$ and $x_2 = 2/3$.

2.7.1 Analytical Solution

For a single barrier potential the BVP (11) can be solved analytically. Assuming that a right-traveling wave of amplitude $\hat{\psi} = 1$ enters the semiconductor at $x = 0$, the wave function reads

$$\psi(x) = \begin{cases} e^{\mathrm{i}\sqrt{2E}x} + re^{-\mathrm{i}\sqrt{2E}x}, & \text{if } x \in [0, x_1), \\ ae^{\mathrm{i}\sqrt{2(E-V_0)}x} + be^{-\mathrm{i}\sqrt{2(E-V_0)}x}, & \text{if } x \in [x_1, x_2), \\ te^{\mathrm{i}\sqrt{2E}x}, & \text{if } x \in [x_2, L]. \end{cases} \tag{45}$$

The coefficients r, a, b and t can be determined by using the continuity argument of the wave function and its first derivative at $x = x_1$ and $x = x_2$. For more details on the computation of the analytical solution including formulas of the coefficients r, a, b and t the interested reader is referred to [13].

Note that the solution of the so-called *transfer-matrix method* coincides with the analytical solution in the case of a single barrier potential, cf. [24].

Since we have three domains of the same length the step size h has to be of the form $h = \frac{1}{3n}$ with $n = 1, 2, \ldots$, so that the discretized domains also have the same length. Otherwise the FDSs would not solve the problem as stated above and the results would differ significantly from the analytical solution.

2.7.2 Numerical Results – The L^2-Error

In this section we present the numerical results of the introduced FDSs and show their discrete L^2-error. The evaluation of the discrete L^2-error, however, is not straightforward for a complex function. Since the numerical results of a stationary problem such as the BVP (11) has an arbitrary phase, we have to optimize the L^2-error with respect to a phase offset $\varphi \in [-\pi, \pi]$. In other words we have to solve the nonlinear problem

$$\Delta\psi_h^{\min} = \min_{\varphi\in[-\pi,\pi]} \Delta\psi_h = \min_{\varphi\in[-\pi,\pi]} \frac{1}{J+1} \sqrt{\sum_{j=0}^{J} |\psi(x_j) - \psi_h(x_j)e^{\mathrm{i}\varphi}|^2}, \tag{46}$$

where ψ denotes the analytical solution and ψ_h is the numerical solution using the step size $h = 1/J$. In order to evaluate the minimal L^2-error $\Delta\psi_h^{\min}$ we discretize the domain $[-\pi, \pi]$ with a step size $h_\varphi = 2\pi/1000$ and analyze the L^2-error $\Delta\psi_h$ at every grid point.

In Fig. 2(a) the L^2-errors $\Delta\psi_h^{\min}$ of the standard FDS and the combined Numerov-Mickens FDS are plotted against the number of grid points $J = 1/h$ for the resonance energy $E = E_{\text{resonance}} \approx 544$. The error of the Numerov FDS and the error of the Mickens FDS coincide with the error of the standard discretization for the level of detail in Fig. 2(a). For these three FDSs the L^2-error is in $\mathcal{O}(h^2)$. The L^2-error of the combined Numerov-Mickens FDS, however, is only in $\mathcal{O}(h)$.

Fig. 2(b) shows that the phase shift adjusted L^2-errors of the Numerov FDS almost coincides with the standard FDS and the Mickens FDS, i.e. the Numerov FDS turns out to be not of higher order than the standard FDS and the Mickens FDS. Although the higher order of the Numerov FDS is considered to be an advantage compared to the standard FDS and the Mickens FDS, it is this property that leads to the observed error of the scheme. By applying the identity

$$\psi_{xx} = \left(\left(\frac{\psi_x}{\psi} \right)_x + \left(\frac{\psi_x}{\psi} \right)^2 \right) \psi$$

to the Schrödinger equation (1) we get

$$\left(\frac{\psi_x}{\psi} \right)_x + \left(\frac{\psi_x}{\psi} \right)^2 = V(x) - E. \tag{47}$$

Under the assumption of the Numerov FDS, i.e. that the discretization is of fourth order, the left hand side of Eq. (47) is second order differentiable. The right hand side, however, is not second order differentiable as the potential V comprises two jump discontinuities at the barrier's ends. For the standard discretization, the left hand side of Eq. (47) is continuous but not necessarily differentiable. Hence, the jump discontinuities of the potential also lead to an error but we expect this error to be smaller than for the Numerov scheme.

An approach to improve the behavior of the Numerov FDS for a discontinuous potential V is to use the standard FDS of the Schrödinger equation at the point of discontinuity of the potential V and the Numerov FDS elsewhere. Although spurious oscillations due to possible incompatibility of the two schemes cannot be observed, numerical testing shows that the results cannot be improved significantly.

Before continuing with the multiband case, let us note that apart from the list of FDSs we introduced in this section there are a plenty of FDSs that can be used for the stationary linear Schrödinger equation (1). However, the chosen FDSs demonstrate the principle of using FDSs for the Schrödinger equation clearly. The reader is referred to Simos and Williams [26] for a concise review on FDSs for the Schrödinger equation.

3 The General $\mathbf{k}\cdot\mathbf{p}$-Model

In this section introduce the general $\mathbf{k}\cdot\mathbf{p}$-model. Let $d \in \mathbb{N}$ denote the number of considered bands of the semiconductor and $\mathbf{F}(x) \in \mathbb{C}^d$ the vector of the envelope functions $F_1, \ldots, F_d \in \mathbb{C}$. Let $\mathbf{m}(x), \mathbf{e}(x) \in \mathbb{R}^{d\times d}$ be diagonal, real and regular $d \times d$-matrices,

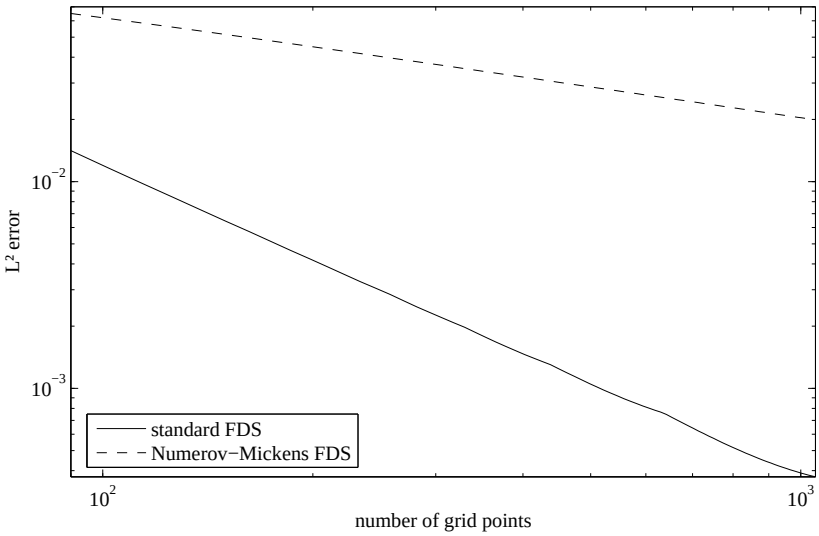

(a) L^2-error of the standard FDS (solid line) and the Numerov-Mickens FDS (dashed line).

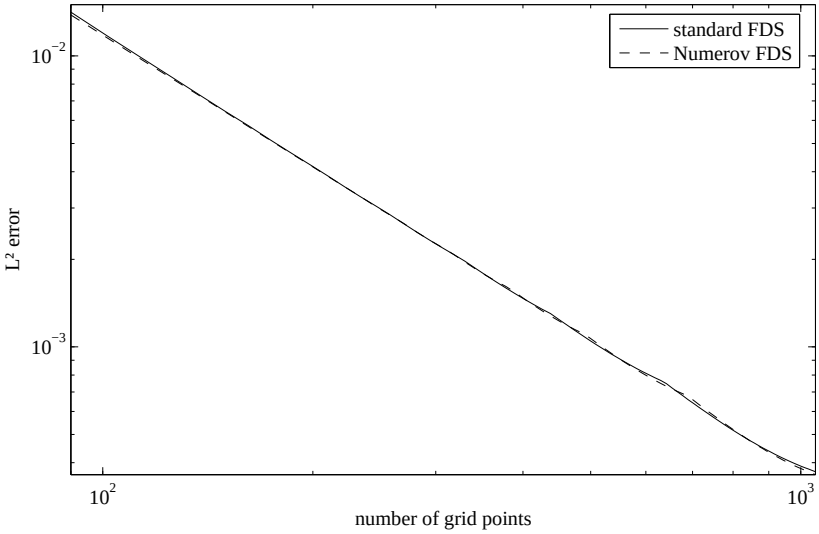

(b) L^2-error of the standard FDS (solid line) and the Numerov FDS (dashed line).

Figure 2: Comparison of the L^2-errors of the numerical schemes for the resonance energy $E = E_{\text{resonance}} \approx 544$. Note that the L^2-errors of the Numerov FDS and the Mickens FDS coincide with the L^2-error of the standard FDS for the used level of detail in (a), while the L^2-error of the Mickens FDS coincides with the L^2-error of the Numerov FDS for the used level of detail in (b).

$\mathbf{U}_p(x), \mathbf{U}_{pq}(x), \mathbf{v}(x) \in \mathbb{C}^{d\times d}$ Hermitian $d \times d$-matrices and $\mathbf{M}_0(x), \mathbf{M}_1(x), \mathbf{M}_2(x) \in \mathbb{C}^{d\times d}$ skew-Hermitian $d \times d$-matrices. Then we will refer to

$$\begin{aligned} E\mathbf{F}(x) = &- \frac{\mathrm{d}}{\mathrm{d}x}\left(\mathbf{m}(x)\frac{\mathrm{d}}{\mathrm{d}x}\mathbf{F}(x)\right) + \mathbf{M}_0(x)\frac{\mathrm{d}}{\mathrm{d}x}\mathbf{F}(x) - \frac{\mathrm{d}}{\mathrm{d}x}\left(\mathbf{M}_0^{\mathrm{H}}(x)\mathbf{F}(x)\right) \\ &+ k_1\left(\mathbf{M}_1(x)\frac{\mathrm{d}}{\mathrm{d}x}\mathbf{F}(x) - \frac{\mathrm{d}}{\mathrm{d}x}\left(\mathbf{M}_1^{\mathrm{H}}(x)\mathbf{F}(x)\right)\right) \\ &+ k_2\left(\mathbf{M}_2(x)\frac{\mathrm{d}}{\mathrm{d}x}\mathbf{F}(x) - \frac{\mathrm{d}}{\mathrm{d}x}\left(\mathbf{M}_2^{\mathrm{H}}(x)\mathbf{F}(x)\right)\right) \\ &+ k_1\mathbf{U}_1(x)\mathbf{F}(x) + k_2\mathbf{U}_2(x)\mathbf{F}(x) \\ &+ k_1^2\mathbf{U}_{11}(x)\mathbf{F}(x) + k_2^2\mathbf{U}_{22}(x)\mathbf{F}(x) + k_1k_2\left(\mathbf{U}_{12}(x) + \mathbf{U}_{21}(x)\right)\mathbf{F}(x) \\ &+ \mathbf{v}(x)\mathbf{F}(x) + \mathbf{e}(x)\mathbf{F}(x), \end{aligned} \tag{48}$$

with $x \in \mathbb{R}$ and $k_1, k_2 \in \mathbb{R}$, as *d-band* $\mathbf{k}\cdot\mathbf{p}$*-Schrödinger equation*, cf. [5]. In order to abbreviate this physical formulation we introduce the skew-Hermitian $d \times d$-matrix

$$\mathbf{M}_{\mathrm{S}}(x) = \mathbf{M}_0(x) + k_1\mathbf{M}_1(x) + k_2\mathbf{M}_2(x), \tag{49a}$$

and the Hermitian $d \times d$-matrix

$$\begin{aligned} \mathbf{V}(x) = &\, k_1\mathbf{U}_1(x) + k_2\mathbf{U}_2(x) \\ &+ k_1^2\mathbf{U}_{11}(x) + k_2^2\mathbf{U}_{22}(x) + k_1k_2\left(\mathbf{U}_{12}(x) + \mathbf{U}_{21}(x)\right) + \mathbf{v}(x) + \mathbf{e}(x). \end{aligned} \tag{49b}$$

Then (48) reads

$$E\mathbf{F}(x) = -\frac{\mathrm{d}}{\mathrm{d}x}\left(\mathbf{m}(x)\frac{\mathrm{d}}{\mathrm{d}x}\mathbf{F}(x)\right) + \mathbf{M}_{\mathrm{S}}(x)\frac{\mathrm{d}}{\mathrm{d}x}\mathbf{F}(x) - \frac{\mathrm{d}}{\mathrm{d}x}\left(\mathbf{M}_{\mathrm{S}}^{\mathrm{H}}(x)\mathbf{F}(x)\right) + \mathbf{V}(x)\mathbf{F}(x), \tag{50}$$

with $x \in \mathbb{R}$.

We consider a semiconductor of length L connected to reservoirs at $x = 0$ and $x = L$. Let us assume that the matrices $\mathbf{m}$, $\mathbf{M}_{\mathrm{S}}$ and $\mathbf{V}$ are constant in the reservoirs with

$$\mathbf{m}(x) \equiv \mathbf{m}_0, \quad \mathbf{M}_{\mathrm{S}}(x) \equiv \mathbf{M}_{\mathrm{S},0}, \quad \mathbf{V}(x) \equiv \mathbf{V}_0 \qquad x \le 0,$$

and

$$\mathbf{m}(x) \equiv \mathbf{m}_L, \quad \mathbf{M}_{\mathrm{S}}(x) \equiv \mathbf{M}_{\mathrm{S},L}, \quad \mathbf{V}(x) \equiv \mathbf{V}_L \qquad x \ge L.$$

3.1 The Exterior Problem and the Dispersion Relation

Let us study the exterior problem of the general $\mathbf{k}\cdot\mathbf{p}$-model. In the exterior domains the matrices $\mathbf{m}$, $\mathbf{M}_{\mathrm{S}}$ and $\mathbf{V}$ are constant. Without loss of generality, we focus on the left exterior domain $x \le 0$ with $\mathbf{m}(x) = \mathbf{m}_0$, $\mathbf{M}_{\mathrm{S}}(x) = \mathbf{M}_{\mathrm{S},0}$ and $\mathbf{V}(x) = \mathbf{V}_0$. Note that the results for the right exterior domain $x \ge L$ can be derived analogously. For simplicity let us omit the subscript 0 in $\mathbf{m}_0$, $\mathbf{M}_{\mathrm{S},0}$ and $\mathbf{V}_0$. With these simplifying assumptions, Eq. (48)

regarded on the half line $x \leq 0$ is a second order system of ODEs with constant coefficients that can be written in the form

$$-\mathbf{N}\frac{\mathrm{d}^2}{\mathrm{d}x^2}\mathbf{F} + \mathrm{i}\mathbf{M}\frac{\mathrm{d}}{\mathrm{d}x}\mathbf{F} + (\mathbf{V} - E\mathbb{1})\,\mathbf{F} = \mathbf{0}, \qquad x \leq 0, \tag{51}$$

with $\mathbf{N} = \mathbf{m}$ and $\mathbf{M} = -\mathrm{i}\mathbf{M}_\mathrm{S} + \mathrm{i}\mathbf{M}_\mathrm{S}^\mathrm{H} = -2\mathrm{i}\mathbf{M}_\mathrm{S}$. Note that $\mathbf{M}$ is Hermitian since $\mathbf{M}_\mathrm{S}$ is skew-Hermitian.

By introducing the substitution $\Phi = \left(\mathbf{F}, \frac{\mathrm{d}}{\mathrm{d}x}\mathbf{F}\right)^\mathrm{T}$ we can reduce Eq. (51) to a first order system of ODEs with constant coefficients

$$\mathbf{A}\frac{\mathrm{d}}{\mathrm{d}x}\Phi = \mathbf{B}\Phi, \qquad x \leq 0, \tag{52}$$

with

$$\mathbf{A} = \begin{pmatrix} \mathbf{M} & \mathrm{i}\mathbf{N} \\ -\mathrm{i}\mathbf{N} & \mathbf{0} \end{pmatrix} \in \mathbb{C}^{(2d)\times(2d)}, \qquad \mathbf{B} = \begin{pmatrix} \mathrm{i}\mathbf{V} - \mathrm{i}E\mathbb{1} & \mathbf{0} \\ \mathbf{0} & -\mathrm{i}\mathbf{N} \end{pmatrix} \in \mathbb{C}^{(2d)\times(2d)}.$$

Zisowsky [28] showed for the transient general $\mathbf{k}\cdot\mathbf{p}$-model that the matrices

$$\mathbf{A}_\mathrm{t} = \mathbf{A}, \qquad \mathbf{B}_\mathrm{t} = \begin{pmatrix} \mathrm{i}\mathbf{V} + s\mathbb{1} & \mathbf{0} \\ \mathbf{0} & -\mathrm{i}\mathbf{N} \end{pmatrix},$$

with the Laplace parameter s of the Laplace-transformed exterior problem, are regular for $\mathrm{Re}(s) > 0$. Moreover she proved a *splitting theorem* saying that the matrix $\mathbf{A}_\mathrm{t}^{-1}\mathbf{B}_\mathrm{t}$ has exactly d eigenvalues with positive real part and d eigenvalues with negative real part.

Our aim is to show a similar result for the stationary general $\mathbf{k}\cdot\mathbf{p}$-model (52). First let us show that $\mathbf{A}$ and $\mathbf{B}$ are regular and hence, $\mathbf{A}^{-1}\mathbf{B}$ exists and is also regular. Since $\mathbf{A}_\mathrm{t} = \mathbf{A}$, the matrix $\mathbf{A}$ is regular and $\mathbf{A}^{-1}\mathbf{B}$ exists. Since $\mathbf{V}$ is Hermitian, it is diagonalizable with the real eigenvalues $v_1, \ldots, v_d$. Let us suppose that the energy E satisfies $E \neq v_p$, for $p = 1, \ldots, d$, then the matrix $\mathrm{i}\mathbf{V} - \mathrm{i}E\mathbb{1}$ is similar to $\mathrm{diag}\left(\mathrm{i}\left(v_1 - E\right), \ldots, \mathrm{i}\left(v_d - E\right)\right)$ which is regular. Considering that $\mathbf{N}$ is regular, the matrix $\mathbf{B}$ is regular and hence, the matrix $\mathbf{A}^{-1}\mathbf{B}$ is regular.

Thus, we can write Eq. (52) in the form

$$\frac{\mathrm{d}}{\mathrm{d}x}\Phi = \mathbf{A}^{-1}\mathbf{B}\Phi, \qquad x \leq 0, \tag{53}$$

with

$$\mathbf{A}^{-1}\mathbf{B} = \begin{pmatrix} \mathbf{0} & \mathbb{1} \\ \mathbf{N}^{-1}\left(\mathbf{V} - E\mathbb{1}\right) & \mathrm{i}\mathbf{N}^{-1}\mathbf{M} \end{pmatrix} \in \mathbb{C}^{(2d)\times(2d)}. \tag{54}$$

The solution of Eq. (52) takes the form

$$\Phi(x) = \mathbf{a}e^{\kappa x}, \qquad x \leq 0, \tag{55}$$

where $\kappa = \kappa_1, \ldots, \kappa_{2d} \in \mathbb{C}$ denotes an eigenvalue and $\mathbf{a} = \mathbf{a}(\kappa) \in \mathbb{C}^{2d}$ the corresponding eigenvector of the matrix $\mathbf{A}^{-1}\mathbf{B}$. Since the vector of the envelope functions $\mathbf{F}$ is represented

by the first d components of Φ, we introduce the *amplitude* $\hat{\mathbf{F}} \in \mathbb{C}^d$ of $\mathbf{F}$ that contains the first d components of $\mathbf{a}(\kappa) \in \mathbb{C}^{2d}$. Then the vector of the envelope functions $\mathbf{F}$ takes the form

$$\mathbf{F}(x) = \hat{\mathbf{F}} e^{\mathrm{i}kx}, \tag{56}$$

where $k = \hat{k} + \mathrm{i}\check{k} = -\mathrm{i}\kappa$ is called *wave vector* of $\mathbf{F}$ with the *propagation coefficient* $\hat{k}$ and the *attenuation coefficient* $\check{k}$. If the attenuation coefficient $\check{k}$ is zero, we say that $\mathbf{F}$ is traveling, while $\mathbf{F}$ is called evanescent otherwise. Again we shall refer to the vector $\mathbf{F}$ of the envelope functions as *envelope wave* since it can be written in the form of a plane wave.

By applying the solution (55) to the general $\mathbf{k}\cdot\mathbf{p}$-model (48) we get

$$\hat{\mathbf{H}}\hat{\mathbf{F}} = E\hat{\mathbf{F}}, \tag{57}$$

with

$$\hat{\mathbf{H}} = \hat{\mathbf{H}}(k) = k^2\mathbf{N} - k\mathbf{M} + \mathbf{V}. \tag{58}$$

Note that $\hat{\mathbf{H}}$ is Hermitian if k is real.

Now we propose the main theorem of this section.

Theorem 3.1 (Splitting Theorem)**.** *Let n denote the number of positive eigenvalues of $\mathbf{N}$. Then there exists an energy $E_0^{\mathrm{e}} \in \mathbb{R}$ such that for all energies $E > E_0^{\mathrm{e}}$*

(i) there are exactly n positive and n negative wave vectors (i.e. n right and n left-traveling envelope waves),

(ii) there are exactly $2\,(d-n)$ complex wave vectors, $d-n$ with positive imaginary part (i.e. $d-n$ evanescent envelope waves decaying for $x \to \infty$) and $d-n$ with negative imaginary part (i.e. $d-n$ evanescent envelope waves growing for $x \to \infty$).

Moreover, there exists an energy $E_0^{\mathrm{h}} < E_0^{\mathrm{e}}$ such that for all energies $E < E_0^{\mathrm{h}}$

(iii) there are exactly $d-n$ positive and $d-n$ negative wave vectors (i.e. $d-n$ right and $d-n$ left-traveling envelope waves) and

(iv) there are exactly $2n$ complex wave vectors, n with positive imaginary part (i.e. n evanescent envelope waves decaying for $x \to \infty$) and n with negative imaginary part (i.e. n evanescent envelope waves growing for $x \to \infty$).

Numerical evidence strongly supports the validity of this theorem. However, we were unable to prove it analytically. For the simple case $\mathbf{M} = 0$ and $\mathbf{V} = \mathrm{diag}\,(v_1, \ldots, v_d)$ a proof can be found in [13].

Remark 3.2. *In all examples considered, the d amplitudes $\hat{\mathbf{F}}(k)$ that correspond to the n positive wave vectors and the $d-n$ complex wave vectors with positive imaginary part are linearly independent. Moreover, the d amplitudes $\hat{\mathbf{F}}(k)$ associated with the n negative wave vectors and the $d-n$ complex wave vectors with negative imaginary part are linearly independent.*

3.2 Transparent Boundary Conditions

Let us recall the strategy we used for the single-band model in order to derive the TBCs. We considered a traveling envelope wave $\mathbf{F}^{\mathrm{in}}$ with amplitude of norm 1 that enters the computational domain at $x = 0$. This means that depending on the energy E we require the matrix $\mathbf{N}$ to have at least one positive or negative eigenvalue in order to get at least one pair of traveling envelope waves.

Let us from now on assume that the energy E is greater than some lower bound E_0^{e} and hence, the number n of positive eigenvalues of $\mathbf{N}$ is equal to the number of pairs of traveling envelope waves.

If there are two or more pairs of traveling envelope waves, the incoming envelope wave is not unique. In this case we shall consider a unitary superposition of all right-traveling envelope waves to enter the semiconductor at $x = 0$. This means that we have to specify a priori the values of the n coefficients of the superposition of incoming envelope waves.

Let $\hat{k}_{0,l}^+$, $l = 1, \ldots, n$, denote the n positive wave vectors and $\hat{k}_{0,l}^-$, $l = 1, \ldots, n$, the n negative wave vectors in the left exterior domain. Moreover, let $\check{k}_{0,l}^+$, $l = 1, \ldots, d-n$, denote the $d-n$ complex wave vectors with positive imaginary part and $\check{k}_{0,l}^-$, $l = 1, \ldots, d-n$, the $d-n$ complex wave vectors with negative imaginary part in the left exterior domain. The wave vectors in the right exterior domain are defined analogously with subscript L instead of 0.

Note that in all considered examples, $\hat{k}_l^+ = -\hat{k}_l^-$, for $l = 1, \ldots, n$, and $\check{k}_l^+ = -\check{k}_l^-$, for $l = 1, \ldots, d-n$.

Let $\hat{\mathbf{F}}_0(k)$ denote the amplitude of norm 1 in the left exterior domain that corresponds to the wave vector k, i.e. the eigenvector of norm 1 of $\hat{\mathbf{H}}(k)$ to the energy eigenvalue E. On the other hand, let $\hat{\mathbf{F}}_L(k)$ denote the corresponding amplitude in the right exterior domain.

Let us consider the superposition of all right-traveling envelope functions

$$\mathbf{F}^{\mathrm{in}} = \sum_{l=1}^{n} \omega_l \hat{\mathbf{F}}_0(\hat{k}_{0,l}^+) e^{\mathrm{i}\hat{k}_{0,l}^+ x}, \qquad x < 0, \tag{59}$$

with the coefficients $\omega_1, \ldots, \omega_n \in \mathbb{C}$ that satisfy the normalization condition $\sum_{l=1}^{n} |\omega_l|^2 = 1$. This incoming superposition of envelope functions is partly reflected at the left boundary at $x = 0$, yielding a superposition of left-traveling and evanescent envelope functions

$$\mathbf{F}^{\mathrm{r}} = \sum_{l=1}^{n} \hat{r}_l \hat{\mathbf{F}}_0(\hat{k}_{0,l}^-) e^{\mathrm{i}\hat{k}_{0,l}^- x} + \sum_{l=1}^{d-n} \check{r}_l \hat{\mathbf{F}}_0(\check{k}_{0,l}^-) e^{\mathrm{i}\check{k}_{0,l}^- x}, \qquad x < 0, \tag{60}$$

with the reflection coefficients $\hat{r}_l$ and $\check{r}_l$. Furthermore, the incoming waves are partly transmitted at the right boundary at $x = L$, which results in a superposition of right-traveling and evanescent envelope functions that takes the form

$$\mathbf{F}^{\mathrm{t}} = \sum_{l=1}^{n} \hat{t}_l \hat{\mathbf{F}}_0(\hat{k}_{0,l}^+) e^{\mathrm{i}\hat{k}_{0,l}^+ x} + \sum_{l=1}^{d-n} \check{t}_l \hat{\mathbf{F}}_0(\check{k}_{0,l}^+) e^{\mathrm{i}\check{k}_{0,l}^+ x}, \qquad x > L, \tag{61}$$

with the transmission coefficients $\hat{t}_l$ and $\check{t}_l$. Thus, the solution in the left exterior domain is

$$\mathbf{F} = \mathbf{F}^{\mathrm{in}} + \mathbf{F}^{\mathrm{r}}, \qquad x < 0, \tag{62}$$

while the solution in the right exterior domain is given by

$$\mathbf{F} = \mathbf{F}^{\mathrm{t}}, \qquad x > L. \tag{63}$$

In order to determine the TBC at the left boundary we evaluate the envelope function $\mathbf{F}$ and its first derivative $\frac{\mathrm{d}}{\mathrm{d}x}\mathbf{F}$ at $x = 0$. We get

$$\mathbf{F}(0) = \sum_{l=1}^{n} \omega_l \hat{\mathbf{F}}_0(\hat{k}_{0,l}^{+}) + \sum_{l=1}^{n} \hat{r}_l \hat{\mathbf{F}}_0(\hat{k}_{0,l}^{-}) + \sum_{l=1}^{d-n} \check{r}_l \hat{\mathbf{F}}_0(\check{k}_{0,l}^{-}) \tag{64a}$$

and

$$\frac{\mathrm{d}}{\mathrm{d}x}\mathbf{F}(0) = \sum_{l=1}^{n} \mathrm{i}\hat{k}_{0,l}^{+} \omega_l \hat{\mathbf{F}}_0(\hat{k}_{0,l}^{+}) + \sum_{l=1}^{n} \mathrm{i}\hat{k}_{0,l}^{-} \hat{r}_l \hat{\mathbf{F}}_0(\hat{k}_{0,l}^{-}) + \sum_{l=1}^{d-n} \mathrm{i}\check{k}_{0,l}^{-} \check{r}_l \hat{\mathbf{F}}_0(\check{k}_{0,l}^{-}). \tag{64b}$$

Let us introduce

$$\mathbf{P}_0 = \begin{pmatrix} \hat{\mathbf{F}}_0(\hat{k}_{0,1}^{-}) & \cdots & \hat{\mathbf{F}}_0(\hat{k}_{0,n}^{-}) & \hat{\mathbf{F}}_0(\check{k}_{0,1}^{-}) & \cdots & \hat{\mathbf{F}}_0(\check{k}_{0,d-n}^{-}) \end{pmatrix} \in \mathbb{C}^{d\times d},$$

and

$$\mathbf{K}_0 = \operatorname{diag}\left(\mathrm{i}\hat{k}_{0,1}^{-}, \ldots, \mathrm{i}\hat{k}_{0,n}^{-}, \mathrm{i}\check{k}_{0,1}^{-}, \ldots, \mathrm{i}\check{k}_{0,d-n}^{-}\right) \in \mathbb{C}^{d\times d},$$

as well as

$$\mathbf{r} = (\hat{r}_1, \ldots, \hat{r}_n, \check{r}_1, \ldots, \check{r}_{d-n})^{\mathrm{T}} \in \mathbb{C}^{d}.$$

Then we can rewrite the envelope wave $\mathbf{F}$ and its first derivative $\frac{\mathrm{d}}{\mathrm{d}x}\mathbf{F}$ at $x = 0$ in the form

$$\mathbf{P}_0\mathbf{r} = \mathbf{F}(0) - \sum_{l=1}^{n} \omega_l \hat{\mathbf{F}}_0(\hat{k}_{0,l}^{+}), \tag{65a}$$

and

$$\mathbf{P}_0\mathbf{K}_0\mathbf{r} = \frac{\mathrm{d}}{\mathrm{d}x}\mathbf{F}(0) - \sum_{l=1}^{n} \mathrm{i}\hat{k}_{0,l}^{+} \omega_l \hat{\mathbf{F}}_0(\hat{k}_{0,l}^{+}). \tag{65b}$$

Since the amplitudes $\hat{\mathbf{F}}_0(\hat{k}_{0,1}^{-}), \ldots, \hat{\mathbf{F}}_0(\hat{k}_{0,n}^{-}), \hat{\mathbf{F}}_0(\check{k}_{0,1}^{-}), \ldots, \hat{\mathbf{F}}_0(\check{k}_{0,d-n}^{-})$ are linearly independent, cf. Remark 3.2, the matrix $\mathbf{P}_0$ is regular and hence, its inverse $\mathbf{P}_0^{-1}$ exists. Then the reflection coefficient vector $\mathbf{r}$ reads

$$\mathbf{r} = \mathbf{P}_0^{-1}\left(\mathbf{F}(0) - \sum_{l=1}^{n} \omega_l \hat{\mathbf{F}}_0(\hat{k}_{0,l}^{+})\right),$$

cf. Eq. (65a). Applied to Eq. (65b) we get the left TBC

$$\mathbf{F}_x(0) - \mathbf{P}_0\mathbf{K}_0\mathbf{P}_0^{-1}\mathbf{F}(0) = \sum_{l=1}^{n}\left(\mathrm{i}\hat{k}_{0,l}^{+}\mathbb{1} - \mathbf{P}_0\mathbf{K}_0\mathbf{P}_0^{-1}\right)\omega_l\hat{\mathbf{F}}_0(\hat{k}_{0,l}^{+}). \tag{66}$$

At the right boundary we proceed analogously. The envelope wave $\mathbf{F}$ and its first derivative $\frac{\mathrm{d}}{\mathrm{d}x}\mathbf{F}$ at $x = L$ read

$$\mathbf{F}(L) = \sum_{l=1}^{n}\hat{t}_l\hat{\mathbf{F}}_L(\hat{k}_{L,l}^{+})e^{\mathrm{i}\hat{k}_{L,l}^{+}L} + \sum_{l=1}^{d-n}\check{t}_l\hat{\mathbf{F}}_L(\check{k}_{L,l}^{+})e^{\mathrm{i}\check{k}_{L,l}^{+}L}, \tag{67a}$$

and

$$\frac{\mathrm{d}}{\mathrm{d}x}\mathbf{F}(L) = \sum_{l=1}^{n}\mathrm{i}\hat{k}_{L,l}^{+}\hat{t}_l\hat{\mathbf{F}}_L(\hat{k}_{L,l}^{+})e^{\mathrm{i}\hat{k}_{L,l}^{+}L} + \sum_{l=1}^{d-n}\mathrm{i}\check{k}_{L,l}^{+}\check{t}_l\hat{\mathbf{F}}_L(\check{k}_{L,l}^{+})e^{\mathrm{i}\check{k}_{L,l}^{+}L}. \tag{67b}$$

Let us introduce

$$\mathbf{P}_L = \Big(\hat{\mathbf{F}}_L(\hat{k}_{L,1}^{+})e^{\mathrm{i}\hat{k}_{L,1}^{+}L}\cdots\hat{\mathbf{F}}_L(\hat{k}_{L,n}^{+})e^{\mathrm{i}\hat{k}_{L,n}^{+}L} \\ \hat{\mathbf{F}}_L(\check{k}_{L,1}^{+})e^{\mathrm{i}\check{k}_{L,1}^{+}L}\cdots\hat{\mathbf{F}}_L(\check{k}_{L,d-n}^{+})e^{\mathrm{i}\check{k}_{L,d-n}^{+}L}\Big) \in \mathbb{C}^{d\times d},$$

and

$$\mathbf{K}_L = \mathrm{diag}\left(\mathrm{i}\hat{k}_{L,1}^{+},\ldots,\mathrm{i}\hat{k}_{L,n}^{+},\mathrm{i}\check{k}_{L,1}^{+},\ldots,\mathrm{i}\check{k}_{L,d-n}^{+}\right) \in \mathbb{C}^{d\times d},$$

as well as

$$\mathbf{t} = \left(\hat{t}_1,\ldots,\hat{t}_n,\check{t}_1,\ldots,\check{t}_{d-n}\right)^{\mathrm{T}} \in \mathbb{C}^{d}.$$

Then we can rewrite the envelope wave $\mathbf{F}$ and its first derivative $\frac{\mathrm{d}}{\mathrm{d}x}\mathbf{F}$ at $x = L$ in the form

$$\mathbf{P}_L\mathbf{t} = \mathbf{F}(L), \tag{68a}$$

and

$$\mathbf{P}_L\mathbf{K}_L\mathbf{t} = \frac{\mathrm{d}}{\mathrm{d}x}\mathbf{F}(L). \tag{68b}$$

Since the amplitudes $\hat{\mathbf{F}}_L(\hat{k}_{L,1}^{+}),\ldots,\hat{\mathbf{F}}_L(\hat{k}_{L,n}^{+}),\hat{\mathbf{F}}_L(\check{k}_{L,1}^{+}),\ldots,\hat{\mathbf{F}}_L(\check{k}_{L,d-n}^{+})$ are linearly independent, cf. Remark 3.2, so are

$$\hat{\mathbf{F}}_L(\hat{k}_{L,1}^{+})e^{\mathrm{i}\hat{k}_{L,1}^{+}L},\ldots,\hat{\mathbf{F}}_L(\hat{k}_{L,n}^{+})e^{\mathrm{i}\hat{k}_{L,n}^{+}L},\hat{\mathbf{F}}_L(\check{k}_{L,1}^{+})e^{\mathrm{i}\check{k}_{L,1}^{+}L},\ldots,\hat{\mathbf{F}}_L(\check{k}_{L,d-n}^{+})e^{\mathrm{i}\check{k}_{L,d-n}^{+}L}$$

and hence, the matrix $\mathbf{P}_L$ is regular and its inverse $\mathbf{P}_L^{-1}$ exists. Then the transmission coefficient vector $\mathbf{t}$ becomes

$$\mathbf{t} = \mathbf{P}_L^{-1}\mathbf{F}(L),$$

cf. Eq. (68a). Applied to Eq. (68b) we get the right TBC

$$\mathbf{F}_x(L) - \mathbf{P}_L\mathbf{K}_L\mathbf{P}_L^{-1}\mathbf{F}(L) = \mathbf{0}. \tag{69}$$

Let us remark that the coefficients $\omega_1, \ldots, \omega_n$ restrict the solution at the left boundary. However, in physical applications, for example the unstrained eight-band $\mathbf{k}\cdot\mathbf{p}$-model of the lowest conduction band and the three top-most valence bands, all doubly degenerate, with $\mathbf{k}_{||} = \mathbf{0}$ we will consider in our numerical examples in Sec. 3.5, one typically considers only a particular incoming wave. In the example mentioned above, we have $n = 2$, for $E > E_0^{\mathrm{e}}$. As indicated, the bands are doubly degenerate. Mathematically, this means that the eigenvalues of $\mathbf{A}^{-1}\mathbf{B}$ are 2-fold degenerate, i.e. there exist d distinct wave vectors k and for every wave vector k there exist two corresponding amplitudes, if the geometric multiplicity equals the algebraic multiplicity which is the case in our example. In this particular example we have so-called *spin-up solutions* and *spin-down solutions*. If we only consider spin-up envelope functions for example, we set the coefficient ω_1 of the incoming spin-up envelope wave to one and the coefficient ω_2 of the incoming spin-down envelope wave to zero. Depending on the band edge profile the resulting transmitted envelope waves may also consist of spin-down solutions.

3.3 Discretization

We recall the uniform grid $x_j = jh,\ j = 0, \ldots, J$ with $L = Jh$, of the computational interval $(0, L)$ with $\mathbf{N}_j = \mathbf{N}(x_j)$, $\mathbf{M}_{\mathrm{S}j} = \mathbf{M}_{\mathrm{S}}(x_j)$, $\mathbf{V}_j = \mathbf{V}(x_j)$ and the approximation $\mathbf{F}_j \approx \mathbf{F}(x_j)$, $j = 0, \ldots, J$. In order to discretize the general $\mathbf{k}\cdot\mathbf{p}$-model (48) we apply the second order centered difference operator $\mathrm{D}_h^{\mathrm{cen}}$ as well as the standard second order difference operator D_h^{std} to the abbreviated continuous formulation of the general $\mathbf{k}\cdot\mathbf{p}$-model (48)

$$E\mathbf{F} = -\mathbf{N}\mathbf{F}_{xx} + \left(-\mathbf{N}_x + 2\mathbf{M}_{\mathrm{S}}\right)\mathbf{F}_x + \left(\mathbf{V} - \mathbf{M}_{\mathrm{S}\,x}^{\mathrm{H}}\right)\mathbf{F}, \tag{70}$$

for $x \in (0, L)$.

Thus the discretization of the general $\mathbf{k}\cdot\mathbf{p}$-model leads to

$$E\mathbf{F}_j = -\mathbf{N}_j \mathrm{D}_h^{\mathrm{std}}\mathbf{F}_j + \left(-\mathrm{D}_h^{\mathrm{cen}}\mathbf{N}_j + 2\mathbf{M}_{\mathrm{S}j}\right)\mathrm{D}_h^{\mathrm{cen}}\mathbf{F}_j + \left(\mathbf{V}_j - \mathrm{D}_h^{\mathrm{cen}}\mathbf{M}_{\mathrm{S}\,j}^{\mathrm{H}} - E\mathbb{1}\right)\mathbf{F}_j, \tag{71}$$

with $j = 1, \ldots, J-1$, which implies

$$\begin{aligned} E\mathbf{F}_j = &\left(-\frac{1}{h^2}\mathbf{N}_j + \frac{1}{2h}\left(-\frac{1}{2h}\left(\mathbf{N}_{j+1} - \mathbf{N}_{j-1}\right) + 2\mathbf{M}_{\mathrm{S}j}\right)\right)\mathbf{F}_{j+1} \\ &+ \left(\frac{2}{h^2}\mathbf{N}_j + \mathbf{V}_j - \frac{1}{2h}\left(\mathbf{M}_{\mathrm{S}\,j+1}^{\mathrm{H}} - \mathbf{M}_{\mathrm{S}\,j-1}^{\mathrm{H}}\right)\right)\mathbf{F}_j \\ &+ \left(-\frac{1}{h^2}\mathbf{N}_j - \frac{1}{2h}\left(-\frac{1}{2h}\left(\mathbf{N}_{j+1} - \mathbf{N}_{j-1}\right) + 2\mathbf{M}_{\mathrm{S}j}\right)\right)\mathbf{F}_{j-1}, \end{aligned} \tag{72}$$

with $j = 1, \ldots, J-1$.

In the exterior domains $x \leq 0$ and $x \geq L$, the matrices $\mathbf{N}$, $\mathbf{M}_{\mathrm{S}}$ and $\mathbf{V}$ are constant. Without loss of generality we focus on the left exterior domain $x \leq 0$ with $\mathbf{N}(x) = \mathbf{N}_0$, $\mathbf{M}_{\mathrm{S}}(x) = \mathbf{M}_{\mathrm{S},0}$ and $\mathbf{V}(x) = \mathbf{V}_0$. Note that the results for the right exterior domain $x \geq L$

can be derived analogously. For simplicity let us omit the subscript 0 in $\mathbf{N}_0$, $\mathbf{M}_{\mathrm{S},0}$ and $\mathbf{V}_0$. Hence, Eq. (72) is a second order difference equation with constant coefficients of the form

$$E\mathbf{F}_j = \mathbf{M}^+\mathbf{F}_{j+1} + \mathbf{M}^0\mathbf{F}_j + \mathbf{M}^-\mathbf{F}_{j-1}, \qquad j < 0, \tag{73}$$

with

$$\mathbf{M}^+ = -\frac{1}{h^2}\mathbf{N} + \frac{1}{h}\mathbf{M}_{\mathrm{S}}, \qquad \mathbf{M}^0 = \frac{2}{h^2}\mathbf{N} + \mathbf{V}, \qquad \mathbf{M}^- = -\frac{1}{h^2}\mathbf{N} - \frac{1}{h}\mathbf{M}_{\mathrm{S}}. \tag{74}$$

By introducing the substitution $\Phi_j = (\mathbf{F}_j, \mathbf{F}_{j+1})^{\mathrm{T}}$, Eq. (73) can be transformed into a first order difference equation with constant coefficients

$$\mathbf{A}_h\Phi_j = \mathbf{B}_h\Phi_{j-1}, \qquad j < 0, \tag{75}$$

with

$$\mathbf{A}_h = \begin{pmatrix} \mathbb{1} & \mathbf{0} \\ \mathbf{0} & -\mathbf{M}^+ \end{pmatrix}, \qquad \mathbf{B}_h = \begin{pmatrix} \mathbf{0} & \mathbb{1} \\ \mathbf{M}^- & \left(\mathbf{M}^0 - E\mathbb{1}\right) \end{pmatrix}.$$

Note that $\mathbf{M}^+$ and $\mathbf{M}^-$ are not necessarily regular. However, in all examples we examined $\mathbf{M}^+$ and $\mathbf{M}^-$ are regular. In this case, $\mathbf{A}_h$ and $\mathbf{B}_h$ are regular and hence, we can write Eq. (75) in the form

$$\Phi_j = \mathbf{A}_h^{-1}\mathbf{B}_h\Phi_{j-1}, \qquad j < 0,$$

with the regular matrix

$$\mathbf{A}_h^{-1}\mathbf{B}_h = \begin{pmatrix} \mathbf{0} & \mathbb{1} \\ (-\mathbf{M}^+)^{-1}\mathbf{M}^- & (-\mathbf{M}^+)^{-1}\left(\mathbf{M}^0 - E\mathbb{1}\right) \end{pmatrix}.$$

Remark 3.3. *In all examples we examined the geometric multiplicity of the eigenvalues of $\mathbf{A}_h^{-1}\mathbf{B}_h$ is equal to their algebraic multiplicity. Hence, the eigenvectors of $\mathbf{A}_h^{-1}\mathbf{B}_h$ are linearly independent and form a basis of $\mathbb{C}^{4d}$.*

This remark is important in order to use the fact that the first order difference equation (75) with the initial value $\Phi_0 = \mathbf{a}$ has a solution of the form $\Phi_j = \mathbf{a}\alpha^j$, where $\alpha \in \mathbb{C}$ is an eigenvalue of $\mathbf{A}_h^{-1}\mathbf{B}_h$ with corresponding eigenvector $\mathbf{a} \in \mathbb{C}^{2d}$. Thus, we can set the discrete solution at the left boundary to some eigenvector $\mathbf{a}$ of $\mathbf{A}_h^{-1}\mathbf{B}_h$.

The first d components of $\Phi_j \in \mathbb{C}^{2d}$ represent the discrete solution $\mathbf{F}_j \in \mathbb{C}^d$. Therefore, we introduce the *discrete amplitude* $\hat{\mathbf{F}}_h \in \mathbb{C}^d$ that contains the first d components of $\mathbf{a}$. The discrete solution $\mathbf{F}_j$ becomes

$$\mathbf{F}_j = \hat{\mathbf{F}}_h\alpha^j = \hat{\mathbf{F}}_h e^{\mathrm{i}k_h jh}, \tag{76}$$

with the *discrete wave vector* $k_h = \left(\arg(\alpha) - \mathrm{i}\ln|\alpha|\right)/h$.

The discrete solution as given in Eq. (76) implies $\mathbf{F}_{j+1}e^{-\mathrm{i}k_h h} = \mathbf{F}_j = \mathbf{F}_{j-1}e^{\mathrm{i}k_h h}$ and thus, applied to the difference equation (73) we obtain

$$\hat{\mathbf{H}}_h\hat{\mathbf{F}}_h = E\hat{\mathbf{F}}_h, \tag{77}$$

with $\hat{\mathbf{H}}_h = \hat{\mathbf{H}}_h(k_h) = \mathbf{M}^+e^{\mathrm{i}k_h h} + \mathbf{M}^0 + \mathbf{M}^-e^{-\mathrm{i}k_h h}$.

Now we shall state the discrete analogon of Theorem 3.1.

Theorem 3.4 (Discrete Splitting Theorem)**.** *Let n denote the number of positive eigenvalues of $\mathbf{N}$. Then there exists an energy $E^{\mathrm{e}}_{0,h} \in \mathbb{R}$ such that for all energies $E > E^{\mathrm{e}}_{h,0}$*

(i) there are exactly n positive and n negative discrete wave vectors (i.e. n right and n left-traveling discrete envelope waves),

(ii) there are exactly $2\,(d-n)$ complex discrete wave vectors, $d-n$ with positive imaginary part (i.e. $d-n$ evanescent discrete envelope waves decaying for $x \to \infty$) and $d-n$ with negative imaginary part (i.e. $d-n$ evanescent discrete envelope waves growing for $x \to \infty$).

Moreover, there exists an energy $E^{\mathrm{h}}_{h,0} < E^{\mathrm{e}}_{h,0}$ such that for all energies $E < E^{\mathrm{h}}_{h,0}$

(iii) there are exactly $d-n$ positive and $d-n$ negative discrete wave vectors (i.e. $d-n$ right and $d-n$ left-traveling discrete envelope waves) and

(iv) there are exactly $2n$ complex discrete wave vectors, n with positive imaginary part (i.e. n evanescent discrete envelope waves decaying for $x \to \infty$) and n with negative imaginary part (i.e. n evanescent discrete envelope waves growing for $x \to \infty$).

Analogously to Theorem 3.1, numerical evidence strongly supports the validity of this theorem. However, we were unable to prove it analytically.

We already pointed out that in all considered examples the geometric multiplicity of the eigenvalues of $\mathbf{A}_h^{-1}\mathbf{B}_h$ is equal to their algebraic multiplicity and hence, the eigenvectors are linearly independent. In addition, we note

Remark 3.5. *In all considered examples the d discrete amplitudes $\hat{\mathbf{F}}_h(k_h)$ that correspond to the n positive discrete wave vectors and the $d-n$ complex discrete wave vectors with positive imaginary part are linearly independent. Moreover, the d discrete amplitudes $\hat{\mathbf{F}}_h(k_h)$ that are associated with the n negative discrete wave vectors and the $d-n$ complex discrete wave vectors with negative imaginary part are linearly independent.*

3.4 Discrete Transparent Boundary Conditions

In order to derive the DTBCs for the general $\mathbf{k}\cdot\mathbf{p}$-model we apply the discrete solution derived in the previous section to the reflection and transmission conditions (62), (63) and assume that they hold in a small vicinity of the two boundaries, i.e. $j = 0, 1$ and $j = J-1, J$ respectively.

Let us from now on assume that the energy is greater than some lower bound $E^{\mathrm{e}}_{h,0}$ and hence, the number n of positive eigenvalues of $\mathbf{N}$ is equal to the number of purely imaginary, complex conjugate pairs of discrete wave vectors.

Suppose that there is at least one pair of discrete traveling envelope functions, in other words $n \geq 1$. If $n \geq 2$, then we have two or more pairs of traveling envelope functions and hence, the incoming envelope function is not unique. In this case we shall proceed accordingly to the derivation of the TBCs and consider a unitary superposition of all discrete right-traveling envelope functions weighted by the coefficients $\omega_1, \ldots, \omega_n \in \mathbb{C}$.

Let $\hat{k}^+_{h,0,l}$, $l = 1, \dots, n$, denote the n positive discrete wave vectors and $\hat{k}^-_{h,0,l}$, $l = 1, \dots, n$, the n negative discrete wave vectors in the left exterior domain. Moreover, the $d-n$ complex discrete wave vectors with positive imaginary part in the left exterior domain are called $\check{k}^+_{h,0,l}$, $l = 1, \dots, d-n$, and the $d-n$ complex discrete wave vectors with negative imaginary part are denoted by $\check{k}^-_{h,0,l}$, $l = 1, \dots, d-n$. The discrete wave vectors in the right exterior domain are defined analogously with subscript L instead of 0.

In all considered examples we have $\hat{k}^+_{h,l} = -\hat{k}^-_{h,l}$, for $l = 1, \dots, n$, and $\check{k}^+_{h,l} = -\check{k}^-_{h,l}$, for $l = 1, \dots, d-n$.

Let $\hat{\mathbf{F}}_{h,0}(k_h)$ denote the amplitude of norm 1 in the left exterior domain that corresponds to the discrete wave vector k_h, i.e. the eigenvector of norm 1 of $\hat{\mathbf{H}}_h(k_h)$ to the energy eigenvalue E. On the other hand, let $\hat{\mathbf{F}}_{h,L}(k_h)$ be the corresponding amplitude in the right exterior domain.

Then we have

$$\mathbf{F}_j = \mathbf{F}_j^{\mathrm{in}} + \mathbf{F}_j^{\mathrm{r}} = \sum_{l=1}^{n} \omega_l \hat{\mathbf{F}}_{h,0}(\hat{k}^+_{h,0,l}) e^{\mathrm{i}\hat{k}^+_{h,0,l} jh} + \sum_{l=1}^{n} \hat{r}_{h,l} \hat{\mathbf{F}}_{h,0}(\hat{k}^-_{h,0,l}) e^{\mathrm{i}\hat{k}^-_{h,0,l} jh} + \sum_{l=1}^{d-n} \check{r}_{h,l} \hat{\mathbf{F}}_{h,0}(\check{k}^-_{h,0,l}) e^{\mathrm{i}\check{k}^-_{h,0,l} jh},$$

at the left boundary, i.e. for $j = 0, 1$, and

$$\mathbf{F}_j = \mathbf{F}_j^{\mathrm{t}} = \sum_{l=1}^{n} \hat{t}_h \hat{\mathbf{F}}_{h,L}(\hat{k}^+_{h,L,l}) e^{\mathrm{i}\hat{k}^+_{h,L,l} jh} + \sum_{l=1}^{d-n} \check{t}_h \hat{\mathbf{F}}_{h,L}(\check{k}^+_{h,L,l}) e^{\mathrm{i}\check{k}^+_{h,L,l} jh},$$

at the right boundary, i.e. for $j = J-1, J$.

Let us introduce

$$\mathbf{P}_{h,0} = \left(\hat{\mathbf{F}}_{h,0}(\hat{k}^-_{h,0,1}) \quad \cdots \quad \hat{\mathbf{F}}_{h,0}(\hat{k}^-_{h,0,n}) \quad \hat{\mathbf{F}}_{h,0}(\check{k}^-_{h,0,1}) \quad \cdots \quad \hat{\mathbf{F}}_{h,0}(\check{k}^-_{h,0,d-n}) \right) \in \mathbb{C}^{d \times d},$$

and

$$\mathbf{K}_{h,0} = \operatorname{diag}\left(e^{\mathrm{i}\hat{k}^-_{h,0,1} h}, \dots, e^{\mathrm{i}\hat{k}^-_{h,0,n} h}, e^{\mathrm{i}\check{k}^-_{h,0,1} h}, \dots, e^{\mathrm{i}\check{k}^-_{h,0,d-n} h} \right) \in \mathbb{C}^{d \times d},$$

as well as

$$\mathbf{r}_h = (\hat{r}_{h,1}, \dots, \hat{r}_{h,n}, \check{r}_{h,1}, \dots, \check{r}_{h,d-n})^{\mathrm{T}} \in \mathbb{C}^d.$$

Then we can rewrite the discrete envelope function $\mathbf{F}_j$ for $j = 0, 1$ in the form

$$\mathbf{P}_{h,0} \mathbf{r}_h = \mathbf{F}_0 - \sum_{l=1}^{n} \omega_l \hat{\mathbf{F}}_{h,0}(\hat{k}^+_{h,0,l}), \tag{78a}$$

and

$$\mathbf{P}_{h,0} \mathbf{K}_{h,0} \mathbf{r}_h = \mathbf{F}_1 - \sum_{l=1}^{n} \omega_l \hat{\mathbf{F}}_{h,0}(\hat{k}^+_{h,0,l}) e^{\mathrm{i}\hat{k}^+_{h,0,l} h}. \tag{78b}$$

Since $\hat{\mathbf{F}}_{h,0}(\hat{k}^-_{h,0,1}),\dots,\hat{\mathbf{F}}_{h,0}(\hat{k}^-_{h,0,n})$ and $\hat{\mathbf{F}}_{h,0}(\check{k}^-_{h,0,1}),\dots,\hat{\mathbf{F}}_{h,0}(\check{k}^-_{h,0,d-n})$ are linearly independent, cf. Remark 3.5, the matrix $\mathbf{P}_{h,0}$ is regular and hence, its inverse $\mathbf{P}_{h,0}^{-1}$ exists. Then the reflection coefficient vector $\mathbf{r}_h$ is given by

$$\mathbf{r}_h = \mathbf{P}_{h,0}^{-1}\left(\mathbf{F}_0 - \sum_{l=1}^{n}\omega_l\hat{\mathbf{F}}_{h,0}(\hat{k}^+_{h,0,l})\right),$$

cf. Eq. (78a). Applied to Eq. (78b) we get the left DTBC

$$\mathbf{F}_1 - \mathbf{P}_{h,0}\mathbf{K}_{h,0}\mathbf{P}_{h,0}^{-1}\mathbf{F}_0 = \sum_{l=1}^{n}\left(e^{\mathrm{i}\hat{k}^+_{h,0,l}}\mathbb{1} - \mathbf{P}_{h,0}\mathbf{K}_{h,0}\mathbf{P}_{h,0}^{-1}\right)\omega_l\hat{\mathbf{F}}_{h,0}(\hat{k}^+_{h,0,l}), \tag{79}$$

compared to the left TBC (66).

At the right boundary we proceed analogously. Let us introduce

$$\mathbf{P}_{h,L} = \begin{pmatrix}\hat{\mathbf{p}}_1\cdots\hat{\mathbf{p}}_n & \check{\mathbf{p}}_1\cdots\check{\mathbf{p}}_{d-n}\end{pmatrix} \in \mathbb{C}^{d\times d},$$

with the columns $\hat{\mathbf{p}}_l = \hat{\mathbf{F}}_{h,L}(\hat{k}^+_{h,L,l})e^{\mathrm{i}\hat{k}^+_{h,L,l}hJ}$ and $\check{\mathbf{p}}_l = \hat{\mathbf{F}}_{h,L}(\check{k}^+_{h,L,l})e^{\mathrm{i}\check{k}^+_{h,L,l}hJ}$. Moreover, we introduce

$$\mathbf{K}_{h,L} = \operatorname{diag}\left(e^{-\mathrm{i}\hat{k}^+_{h,L,1}h},\dots,e^{-\mathrm{i}\hat{k}^+_{h,L,n}h},e^{-\mathrm{i}\check{k}^+_{h,L,1}h},\dots,e^{-\mathrm{i}\check{k}^+_{h,L,d-n}h}\right) \in \mathbb{C}^{d\times d},$$

as well as

$$\mathbf{t}_h = \left(\hat{t}_{h,1},\dots,\hat{t}_{h,n},\check{t}_{h,1},\dots,\check{t}_{h,d-n}\right)^{\mathrm{T}} \in \mathbb{C}^d.$$

Then we can rewrite the discrete envelope function $\mathbf{F}_j$ for $j = J-1, J$ in the form

$$\mathbf{P}_{h,L}\mathbf{t}_h = \mathbf{F}_J, \tag{80a}$$

and

$$\mathbf{P}_{h,L}\mathbf{K}_{h,L}\mathbf{t}_h = \mathbf{F}_{J-1}. \tag{80b}$$

Since the discrete amplitudes $\hat{\mathbf{F}}_{h,L}(\hat{k}^+_{h,L,1}),\dots,\hat{\mathbf{F}}_{h,L}(\hat{k}^+_{h,L,n})$ and $\hat{\mathbf{F}}_{h,L}(\check{k}^+_{h,L,1}),\dots,\hat{\mathbf{F}}_{h,L}(\check{k}^+_{h,L,d-n})$ are linearly independent, cf. Remark 3.5, so are $\hat{\mathbf{F}}_{h,L}(\hat{k}^+_{h,L,1})e^{\mathrm{i}\hat{k}^+_{h,L,1}hJ},\dots,\hat{\mathbf{F}}_{h,L}(\hat{k}^+_{h,L,n})e^{\mathrm{i}\hat{k}^+_{h,L,n}hJ}$ and $\hat{\mathbf{F}}_{h,L}(\check{k}^+_{h,L,1})e^{\mathrm{i}\check{k}^+_{h,L,1}hJ},\dots,\hat{\mathbf{F}}_{h,L}(\check{k}^+_{h,L,d-n})e^{\mathrm{i}\check{k}^+_{h,L,d-n}hJ}$. Thus, the matrix $\mathbf{P}_{h,L}$ is regular and its inverse $\mathbf{P}_{h,L}^{-1}$ exists. Then the transmission coefficient vector $\mathbf{t}_h$ reads

$$\mathbf{t}_h = \mathbf{P}_{h,L}^{-1}\mathbf{F}_J,$$

cf. Eq. (80a). Applied to Eq. (80b) we get the right DTBC

$$\mathbf{F}_{J-1} - \mathbf{P}_{h,L}\mathbf{K}_{h,L}\mathbf{P}_{h,L}^{-1}\mathbf{F}_J = \mathbf{0}, \tag{81}$$

in contrast to the right TBC (69).

3.5 Numerical Examples

3.5.1 The Free Scattering State

In our first example, we want to examine the numerical result of an unstrained eight-band $\mathbf{k}\cdot\mathbf{p}$-model of the lowest conduction band and the three top-most valence bands, all doubly degenerate, with $\mathbf{k}_{||} = \mathbf{0}$, in the case of the free scattering state and compare it with the analytical solution, that can be derived from the results in Sec. 3.1.

In this case the 8×8-$\mathbf{k}\cdot\mathbf{p}$-Hamiltonian reduces to

$$\mathbf{H} = \mathbf{H}_0 + \mathbf{H}_\Delta + \mathbf{H}_1 \frac{\mathrm{d}}{\mathrm{d}x} + \mathbf{H}_2 \frac{\mathrm{d}^2}{\mathrm{d}x^2}, \tag{82}$$

where $\mathbf{H}_0$ describes the *band edge profile*, $\mathbf{H}_\Delta$ denotes the *spin orbit coupling*, $\mathbf{H}_1$ contains all *first order couplings*, i.e. the inter-band couplings, and $\mathbf{H}_2$ contains all *second order couplings*, i.e. the intra-band couplings, see [12].

The band edge profile is given by

$$\mathbf{H}_0 = \operatorname{diag}\left(E_\mathrm{c}, E_\mathrm{v}, E_\mathrm{v}, E_\mathrm{v}, E_\mathrm{c}, E_\mathrm{v}, E_\mathrm{v}, E_\mathrm{v}\right) \in \mathbb{R}^{8\times 8}, \tag{83}$$

where E_c is the conduction band edge and E_v is the valence band edge with the $E_\mathrm{g} = E_\mathrm{c} - E_\mathrm{v}$.

The spin orbit coupling matrix $\mathbf{H}_\Delta \in \mathbb{C}^{8\times 8}$ takes the form

$$\mathbf{H}_\Delta = \frac{\Delta_\mathrm{so}}{3} \begin{pmatrix} \mathbf{G} + \mathrm{i}\mathbf{G}_z & \mathbf{G}_y + \mathrm{i}\mathbf{G}_x \\ -\mathbf{G}_y + \mathrm{i}\mathbf{G}_x & \mathbf{G}_\mathrm{so} - \mathrm{i}\mathbf{G}_z \end{pmatrix}, \tag{84}$$

with $\mathbf{G}_\mathrm{so} = \operatorname{diag}\left(0, -1, -1, -1\right) \in \mathbb{R}^{4\times 4}$ and $\mathbf{G}_x, \mathbf{G}_y, \mathbf{G}_z \in \mathbb{R}^{4\times 4}$ defined by $\left(\mathbf{G}_x\right)_{ij} = \delta^{i,4}\delta^{j,3} - \delta^{i,3}\delta^{j,4}$, $\left(\mathbf{G}_y\right)_{ij} = \delta^{i,2}\delta^{j,4} - \delta^{i,4}\delta^{j,2}$, $\left(\mathbf{G}_z\right)_{ij} = \delta^{i,3}\delta^{j,2} - \delta^{i,2}\delta^{j,3}$, where $\delta^{i,j}$ is the usual Kronecker symbol with $\delta^{i,j} = 1$ if $i = j$ and $\delta^{i,j} = 0$ otherwise. The parameter Δ_so denotes the so-called *spin orbit splitting*.

The matrix $\mathbf{H}_1 \in \mathbb{R}^{8\times 8}$ of first order couplings has components

$$\left(\mathbf{H}_1\right)_{ij} = P_0 \left(\delta^{i,1}\delta^{j,4} - \delta^{i,4}\delta^{j,1} + \delta^{i,8}\delta^{j,5} - \delta^{i,5}\delta^{j,8}\right) \tag{85}$$

while the matrix $\mathbf{H}_2 \in \mathbb{C}^{8\times 8}$ of second order couplings takes the form

$$\mathbf{H}_2 = -\operatorname{diag}\left(\alpha, \mu, \mu, \lambda, \alpha, \mu, \mu, \lambda\right), \tag{86}$$

where the coefficients $\alpha, \lambda, \mu \in \mathbb{C}$ are given by

$$\alpha = \frac{\hbar^2}{2m_\mathrm{c}} - \frac{P_0^2}{E_\mathrm{g}} \frac{E_\mathrm{g} + 2\frac{\Delta_\mathrm{so}}{3}}{E_\mathrm{g} + \Delta_\mathrm{so}}, \quad \lambda = \frac{P_0^2}{E_\mathrm{g}} - \frac{\hbar^2}{2m_0}\left(\gamma_1 + 4\gamma_2\right), \quad \mu = -\frac{\hbar^2}{2m_0}\left(\gamma_1 - 2\gamma_2\right),$$

with the effective mass m_c of the conduction band and the *Luttinger parameters* γ_1 and γ_2.

Written in the usual notation

$$-\mathbf{N}\frac{\mathrm{d}^2}{\mathrm{d}x^2}\mathbf{F} + \mathrm{i}\mathbf{M}\frac{\mathrm{d}}{\mathrm{d}x}\mathbf{F} + (\mathbf{V} - E\mathbb{1})\,\mathbf{F} = \mathbf{0}, \tag{87}$$

cf. Eq. (51), we have $\mathbf{N} = -\mathbf{H}_2$, $\mathbf{M} = -\mathrm{i}\mathbf{H}_1$ and $\mathbf{V} = \mathbf{H}_0 + \mathbf{H}_\Delta$.

For simplicity, we set $\hbar = m_0 = 1$ as well as $L = 1$. We use the dimensionless version of the parameters as given in [14] that are given by $\alpha = 3.32$, $\lambda = -18.77$, $\mu = -3.24$, $P_0 = 132.744$ and $\Delta_{\mathrm{so}} = 419.07$. According to [14], we set the band edges to $E_{\mathrm{c}} = 905.96$ and $E_{\mathrm{v}} = 0$.

For these settings and a step size $h = 1/50$ Fig. 3 shows the analytical and discrete dispersion relations. The discrete dispersion relation is $2\frac{\pi}{h}$-periodic and the positive trunk of the discrete dispersion relation for these particular settings is injective in $[0, \pi/h]$. Thus, there does not exist an energy window such that we expect spurious oscillations for all admissible energies outside this window due to the wrong choice of the discrete wave vectors.

In the comparison of the numerical and analytical solution we observe a small phase error in the numerical solution. This error decreases for smaller step sizes which can be seen from the discrete L^2-error. Recall that the discrete L^2-error is the solution of the nonlinear optimization problem

$$\Delta\mathbf{F}_h^{\min} = \min_{\varphi\in[-\pi,\pi]} \Delta\mathbf{F}_h = \min_{\varphi\in[-\pi,\pi]} \frac{1}{J+1}\sqrt{\sum_{j=0}^{J} \|\mathbf{F}(x_j) - \mathbf{F}_j e^{\mathrm{i}\varphi}\|^2}, \tag{88}$$

where $\mathbf{F}(x_j)$ denotes the analytical solution at $x = x_j$ and $\mathbf{F}_j$ the numerical solution using the step size $h = 1/J$. The discrete L^2-error is in $\mathcal{O}(h^2)$ which coincides with the formal order of the standard and centered difference operator we used in order to discretize the general $\mathbf{k}\cdot\mathbf{p}$-model.

3.5.2 The Single Barrier Potential

In our second example we want to analyze the numerical results of the unstrained eight-band $\mathbf{k}\cdot\mathbf{p}$-model with $\mathbf{k}_{||} = \mathbf{0}$ in the case of a single barrier potential. We consider a semiconductor of length L that is split into three parts. Let $0 < x_1 < x_2 < L$, then the three subdomains of the semiconductor are defined by $[0, x_1)$, $[x_1, x_2)$ and $[x_2, L]$. The two outer subdomains have the same physical properties and are denoted by $A = [0, x_1) \cup [x_2, L]$, while the inner subdomain is called $B = [x_1, x_2)$.

We use the same problem as in the previous example, but in the domain B we shall set the band edges to $E_{\mathrm{c}}^B = 1169.33$ and $E_{\mathrm{v}}^B = -167.60$, see [14]. Due to physical conventions, we shall refer to this band edge profile as *quantum well structure*.

Analogously to the single band case, we can compute the analytical solution since the matrices $\mathbf{N}$, $\mathbf{M}$ are constant the matrix $\mathbf{V}$ is piecewise constant. Let us denote the matrix $\mathbf{V}$ in the domain A by $\mathbf{V}_A$ and in the domain B by $\mathbf{V}_B$. Suppose that the energy E is greater

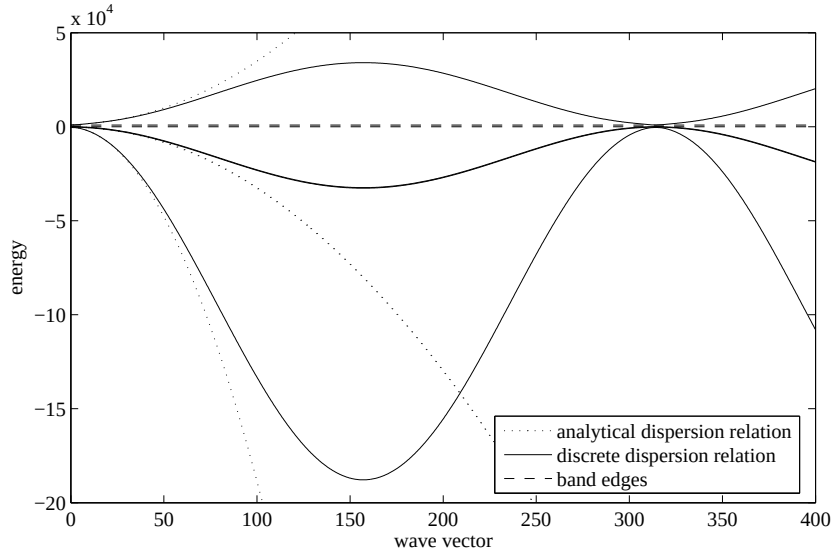

(a) Analytical and discrete dispersion relations.

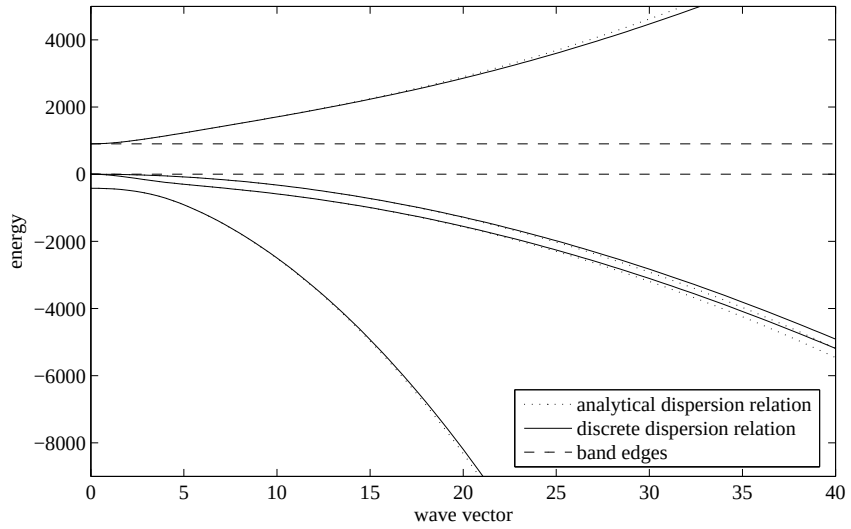

(b) Detail view of (a).

Figure 3: Analytical (dotted line) and discrete (solid line) dispersion relations of the unstrained eight-band $\mathbf{k}\cdot\mathbf{p}$-model with $\mathbf{k}_{||} = \mathbf{0}$. The discrete dispersion relation is plotted for a step size $h = 1/50$.

than some lower bound E_0^{e}, cf. Theorem 3.1. Then the number of positive wave vectors is equal to the number n of positive eigenvalues of N.

Thus, in each domain the envelope function takes the form

$$\mathbf{F}(x) = \sum_{l=1}^{n} \hat{a}_l \hat{\mathbf{F}}(\hat{k}_l^+) e^{\mathrm{i}\hat{k}_l^+ x} + \sum_{l=1}^{d-n} \check{a}_l \hat{\mathbf{F}}(\check{k}_l^+) e^{\mathrm{i}\check{k}_l^+ x} + \sum_{l=1}^{n} \hat{b}_l \hat{\mathbf{F}}(\hat{k}_l^-) e^{\mathrm{i}\hat{k}_l^- x} + \sum_{l=1}^{d-n} \check{b}_l \hat{\mathbf{F}}(\check{k}_l^-) e^{\mathrm{i}\check{k}_l^- x},$$

with the coefficients $\hat{a}_p, \check{a}_q, \hat{b}_p, \check{b}_q \in \mathbb{C}$, with $p = 1, \ldots, n$ and $q = 1, \ldots, d-n$. Here we used the notation of wave vectors and amplitudes we introduced in Sec. 3.2. Note that the amplitudes are of norm 1. In the sequel we will add a subscript A or B to the amplitudes and wave vectors in order to indicate which domain they belong to.

We consider a unitary superposition of all right-traveling envelope functions in A that enters the semiconductor at $x = 0$. Again we shall multiply these n incoming envelope waves with the coefficients $\omega_1, \ldots, \omega_n$. At $x = x_1$ this superposition of envelope functions is partly reflected. On the other hand, we expect a superposition of transmitted envelope functions in the domain $[x_2, L]$ that leaves the semiconductor at $x = L$. Thus, the envelope function reads

$$\mathbf{F}(x) = \begin{cases} \mathbf{F}_{A_1}(x) & \text{if } x \in [0, x_1), \\ \mathbf{F}_B(x) & \text{if } x \in [x_1, x_2), \\ \mathbf{F}_{A_2}(x) & \text{if } x \in [x_2, L], \end{cases} \tag{89}$$

with

$$\begin{aligned}
\mathbf{F}_{A_1}(x) &= \sum_{l=1}^{n} \omega_l \hat{\mathbf{F}}_A(\hat{k}_{A,l}^+) e^{\mathrm{i}\hat{k}_{A,l}^+ x} + \sum_{l=1}^{n} \hat{r}_l \hat{\mathbf{F}}_A(\hat{k}_{A,l}^-) e^{\mathrm{i}\hat{k}_{A,l}^- x} + \sum_{l=1}^{d-n} \check{r}_l \hat{\mathbf{F}}_A(\check{k}_{A,l}^-) e^{\mathrm{i}\check{k}_{A,l}^- x}, \\
\mathbf{F}_B(x) &= \sum_{l=1}^{n} \hat{a}_l \hat{\mathbf{F}}_B(\hat{k}_{B,l}^+) e^{\mathrm{i}\hat{k}_{B,l}^+ x} + \sum_{l=1}^{d-n} \check{a}_l \hat{\mathbf{F}}_B(\check{k}_{B,l}^+) e^{\mathrm{i}\check{k}_{B,l}^+ x} \\
&\quad + \sum_{l=1}^{n} \hat{b}_l \hat{\mathbf{F}}_B(\hat{k}_{B,l}^-) e^{\mathrm{i}\hat{k}_{B,l}^- x} + \sum_{l=1}^{d-n} \check{b}_l \hat{\mathbf{F}}_B(\check{k}_{B,l}^-) e^{\mathrm{i}\check{k}_{B,l}^- x}, \\
\mathbf{F}_{A_2}(x) &= \sum_{l=1}^{n} \hat{t}_l \hat{\mathbf{F}}_A(\hat{k}_{A,l}^+) e^{\mathrm{i}\hat{k}_{A,l}^+ x} + \sum_{l=1}^{d-n} \check{t}_l \hat{\mathbf{F}}_A(\check{k}_{A,l}^+) e^{\mathrm{i}\check{k}_{A,l}^+ x}.
\end{aligned}$$

We know that the solution (89) and its derivative are continuous, cf. [14]. In particular they are continuous at $x = x_1$ and $x = x_2$. Hence, we get a system of linear equations that can be written in the form $\mathbf{Qc} = \mathbf{s}$ with the vector

$$\begin{aligned}
\mathbf{c} = (&\hat{r}_1, \ldots, \hat{r}_n, \check{r}_1, \ldots, \check{r}_{d-n}, \hat{a}_1, \ldots, \hat{a}_n, \check{a}_1, \ldots, \check{a}_{d-n}, \\
&\hat{b}_1, \ldots, \hat{b}_n, \check{b}_1, \ldots, \check{b}_{d-n}, \hat{t}_1, \ldots, \hat{t}_n, \check{t}_1, \ldots, \check{t}_{d-n}\Big)^{\mathrm{T}} \in \mathbb{C}^{4d}
\end{aligned}$$

of the unknowns, the vector

$$\mathbf{s} = \begin{pmatrix} -\sum_{l=1}^{n} \omega_l \hat{\mathbf{F}}_A(\hat{k}^+_{A,l}) e^{\mathrm{i}\hat{k}^+_{A,l}x_1} \\ \mathbf{0} \\ -\sum_{l=1}^{n} \mathrm{i}\hat{k}^+_{A,l}\omega_l \hat{\mathbf{F}}_A(\hat{k}^+_{A,l}) e^{\mathrm{i}\hat{k}^+_{A,l}x_1} \\ \mathbf{0} \end{pmatrix} \in \mathbb{C}^{4d},$$

corresponding to the incoming waves and the coefficient matrix

$$\mathbf{Q} = \begin{pmatrix} \mathbf{Q}_{\hat{r}} & \mathbf{Q}_{\check{r}} & \mathbf{Q}_{\hat{a}} & \mathbf{Q}_{\check{a}} & \mathbf{Q}_{\hat{b}} & \mathbf{Q}_{\check{b}} & \mathbf{Q}_{\hat{t}} & \mathbf{Q}_{\check{t}} \end{pmatrix} \in \mathbb{C}^{4d\times 4d}.$$

The matrices $\mathbf{Q}_{\hat{r}}, \mathbf{Q}_{\hat{a}}, \mathbf{Q}_{\hat{b}}, \mathbf{Q}_{\hat{t}} \in \mathbb{C}^{4d\times n}$ and $\mathbf{Q}_{\check{r}}, \mathbf{Q}_{\check{a}}, \mathbf{Q}_{\check{b}}, \mathbf{Q}_{\check{t}} \in \mathbb{C}^{4d\times(d-n)}$ are given in Appendix A.

We shall not prove mathematically that the matrix $\mathbf{Q}$ is regular. Instead we point out that a singular matrix $\mathbf{Q}$ implies that the homogeneous case of the system of linear equations has a nonzero solution. Thus, there can exist envelope waves inside the computational domain without the existence of an incoming envelope wave which is a physical contradiction. We note that in our particular example the matrix $\mathbf{Q}$ is in fact regular and hence, the unknown coefficients $\hat{r}_p$, $\check{r}_q$, $\hat{a}_p$, $\check{a}_q$, $\hat{b}_p$, $\check{b}_q$, $\hat{t}_p$, $\check{t}_q$, with $p = 1, \ldots, n$ and $q = 1, \ldots, d-n$ are defined uniquely.

Now let us compare the analytical and numerical solutions of the quantum well structure. Fig. 4 shows the norms and phases of the analytical and numerical solutions as well as a schematic view of the band edge profile.

As expected, we do not observe any spurious oscillations. Fig. 3(b) illustrates that for the chosen energy $E = 1500$ there exists a unique positive discrete wave vector in $[0, \pi/h]$. However, we observe a small phase error. This error decreases for smaller step sizes.

In Fig. 5 the analytical and numerical transmission coefficients are plotted against the energy E. As before, the step size $h = 1/150$ is used. Since the curve of the numerical transmission coefficient coincides with the curve of the analytical transmission coefficient for the used level of detail in Fig. 5(a), only the analytical transmission coefficient is plotted. We observe that the qualitative behavior of the transmission coefficient of this particular quantum well structure is similar to the behavior of the transmission coefficient of the single barrier examples in the previous chapters. Note that the first resonance is located at $E \approx 1856$.

Finally, we want to investigate the discrete L^2-error of the numerical scheme. Recall that we have to solve the optimization problem (88). Recall that the L^2-error decayed like $\mathcal{O}(h^2)$ in the free scattering state example, which confirmed the formal order of the numerical scheme. In the quantum well example, however, we observe that the numerical scheme is of order one only.

4 Conclusion

In this chapter we derived DTBCs for stationary MEMAs. We first solved the continuous exterior problem and derived elementary solutions in the exterior domains and defined the

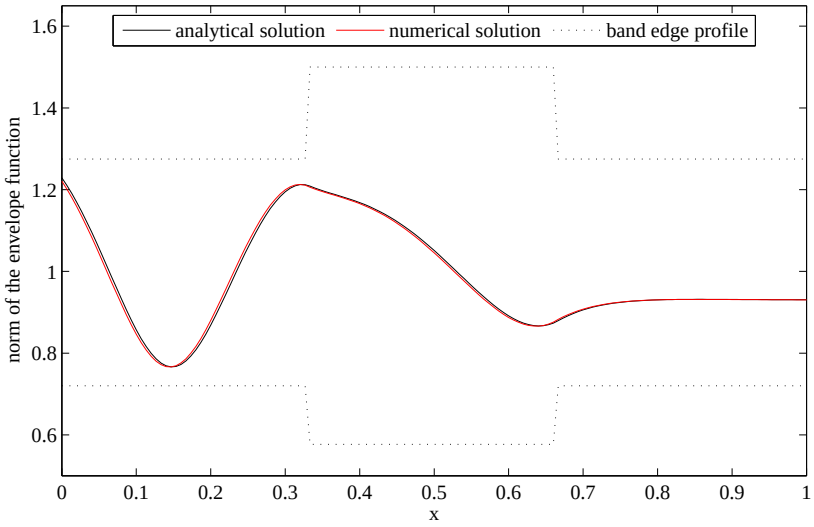

(a) Norm of the analytical and numerical solutions.

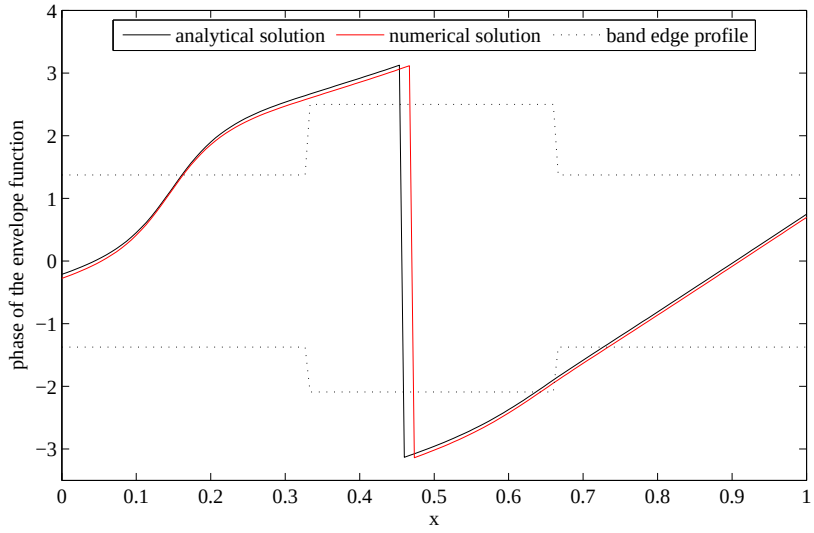

(b) Phases of the analytical and numerical solutions.

Figure 4: Comparison of the analytical solution (black) and the numerical solution (red) of the quantum well structure for a step size $h = 1/150$, an energy $E = 1500$. The dotted line indicates schematically the band end profile.

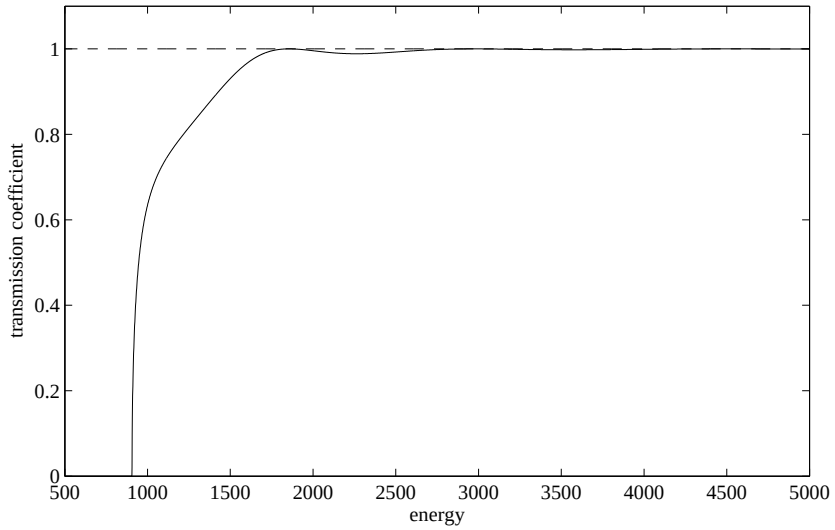

(a) Analytical transmission coefficient.

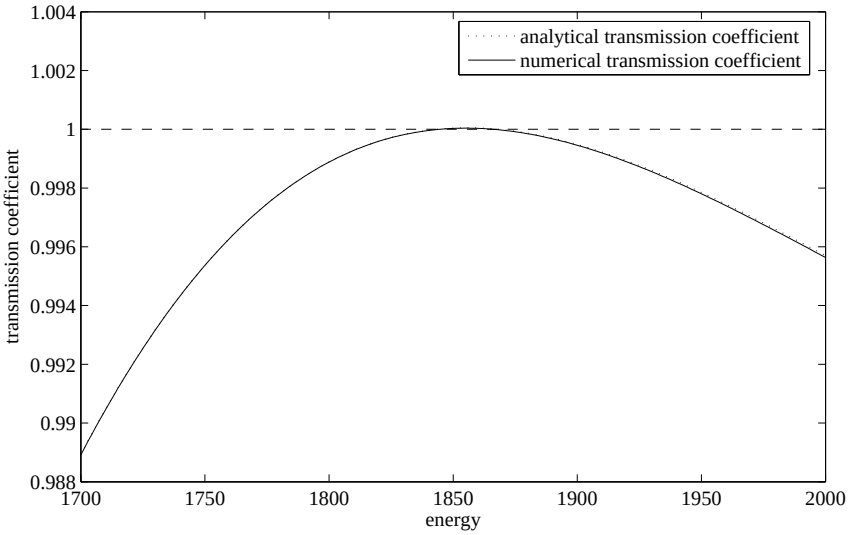

(b) Analytical (dotted line) and numerical (solid line) transmission coefficients near the first resonance at $E \approx 1856$.

Figure 5: Analytical and numerical transmission coefficients of the quantum well structure for a step size $h = 1/150$.

TBCs. After discretizing the underlying BVP and solving the discrete exterior problem, we used the discrete elementary solutions in the exterior domains to derive DTBCs. This fully discrete approach results in reflection-free boundary conditions, while an ad-hoc discretization of the TBCs leads to spurious oscillations of the numerical solution. We tested the numerical schemes and the DTBCs in examples for which an analytical solution can be derived, i.e. for semiconductor nanostructures with piecewise constant band edges.

We reviewed DTBCs for the scalar Schrödinger equation, i.e. the single-band effective mass approximation, and analyzed alternative finite difference schemes. Considering the numerical results we point out that the Mickens FDS is the most promising FDS among the FDSs we introduced for the scalar Schrödinger equation. If the potential is constant the Mickens FDS is an exact FDS and if the potential is not constant it is of order $\mathcal{O}(h^2)$. Which is the best possible order of convergence of the FDSs we introduced since the Numerov FDS which is formally of order $\mathcal{O}(h^4)$ is in fact also only $\mathcal{O}(h^2)$ since it requires the potential to be in $C^2(0,L)$. While the standard FDS and the Numerov FDS are also applicable, the combined Numerov-Mickens FDS, however, leads to significant errors.

We introduced the general d-band $\mathbf{k}\cdot\mathbf{p}$-model, developed the corresponding TBCs and DTBCs, tested them numerically and pointed out that these BCs depend on the choice of the elementary solutions in the exterior domain. It turned out that the numerical scheme when applied to an example with discontinuous band edges is at most of order one.

A topic of future research is the comparison of the introduced methods to solve MEMAs numerically with other methods, such as the transfer matrix method [24, 25] as well as the R-matrix method [27]. In particular, a comparison of these methods is of interest when the analytical solution cannot be derived, such as a quantum barrier structure with added bias.

Simulations of quantum cascade lasers are currently an extensively discussed topic [8]. The current density and the optical gain of quantum cascade lasers can be computed when the envelope functions are known. Based on the DTBCs for MEMAs, developed in this chapter, we plan to perform a fully discrete analysis of these simulations compared to the approach in [20], where an ad-hoc discretization of the TBCs was used.

A Definition of the Coefficient Matrix Q

The matrices $\mathbf{Q}_{\hat{r}}, \mathbf{Q}_{\hat{a}}, \mathbf{Q}_{\hat{b}}, \mathbf{Q}_{\hat{t}} \in \mathbb{C}^{4d\times n}$ and $\mathbf{Q}_{\check{r}}, \mathbf{Q}_{\check{a}}, \mathbf{Q}_{\check{b}}, \mathbf{Q}_{\check{t}} \in \mathbb{C}^{4d\times(d-n)}$ building the coefficient matrix

$$\mathbf{Q} = \begin{pmatrix} \mathbf{Q}_{\hat{r}} & \mathbf{Q}_{\check{r}} & \mathbf{Q}_{\hat{a}} & \mathbf{Q}_{\check{a}} & \mathbf{Q}_{\hat{b}} & \mathbf{Q}_{\check{b}} & \mathbf{Q}_{\hat{t}} & \mathbf{Q}_{\check{t}} \end{pmatrix} \in \mathbb{C}^{4d\times 4d}$$

of the single potential barrier problem in Section 3 are defined by

$$\mathbf{Q}_{\hat{r}} = \begin{pmatrix} \hat{\mathbf{F}}_A(\hat{k}^-_{A,1})e^{\mathrm{i}\hat{k}^-_{A,1}x_1} & \cdots & \hat{\mathbf{F}}_A(\hat{k}^-_{A,n})e^{\mathrm{i}\hat{k}^-_{A,n}x_1} \\ \mathbf{0} & \cdots & \mathbf{0} \\ \mathrm{i}\hat{k}^-_{A,1}\hat{\mathbf{F}}_A(\hat{k}^-_{A,1})e^{\mathrm{i}\hat{k}^-_{A,1}x_1} & \cdots & \mathrm{i}\hat{k}^-_{A,n}\hat{\mathbf{F}}_A(\hat{k}^-_{A,n})e^{\mathrm{i}\hat{k}^-_{A,n}x_1} \\ \mathbf{0} & \cdots & \mathbf{0} \end{pmatrix}$$

$$\mathbf{Q}_{\check{r}} = \begin{pmatrix} \hat{\mathbf{F}}_A(\check{k}^-_{A,1})e^{\mathrm{i}\check{k}^-_{A,1}x_1} & \cdots & \hat{\mathbf{F}}_A(\check{k}^-_{A,d-n})e^{\mathrm{i}\check{k}^-_{A,d-n}x_1} \\ \mathbf{0} & \cdots & \mathbf{0} \\ \mathrm{i}\check{k}^-_{A,1}\hat{\mathbf{F}}_A(\check{k}^-_{A,1})e^{\mathrm{i}\check{k}^-_{A,1}x_1} & \cdots & \mathrm{i}\check{k}^-_{A,d-n}\hat{\mathbf{F}}_A(\check{k}^-_{A,d-n})e^{\mathrm{i}\check{k}^-_{A,d-n}x_1} \\ \mathbf{0} & \cdots & \mathbf{0} \end{pmatrix}$$

$$\mathbf{Q}_{\hat{a}} = \begin{pmatrix} -\hat{\mathbf{F}}_B(\hat{k}^+_{B,1})e^{\mathrm{i}\hat{k}^+_{B,1}x_1} & \cdots & -\hat{\mathbf{F}}_B(\hat{k}^+_{B,n})e^{\mathrm{i}\hat{k}^+_{B,n}x_1} \\ \hat{\mathbf{F}}_B(\hat{k}^+_{B,1})e^{\mathrm{i}\hat{k}^+_{B,1}x_2} & \cdots & \hat{\mathbf{F}}_B(\hat{k}^+_{B,n})e^{\mathrm{i}\hat{k}^+_{B,n}x_2} \\ -\mathrm{i}\hat{k}^+_{B,1}\hat{\mathbf{F}}_B(\hat{k}^+_{B,1})e^{\mathrm{i}\hat{k}^+_{B,1}x_1} & \cdots & -\mathrm{i}\hat{k}^+_{B,n}\hat{\mathbf{F}}_B(\hat{k}^+_{B,n})e^{\mathrm{i}\hat{k}^+_{B,n}x_1} \\ \mathrm{i}\hat{k}^+_{B,1}\hat{\mathbf{F}}_B(\hat{k}^+_{B,1})e^{\mathrm{i}\hat{k}^+_{B,1}x_2} & \cdots & \mathrm{i}\hat{k}^+_{B,n}\hat{\mathbf{F}}_B(\hat{k}^+_{B,n})e^{\mathrm{i}\hat{k}^+_{B,n}x_2} \end{pmatrix}$$

$$\mathbf{Q}_{\check{a}} = \begin{pmatrix} -\hat{\mathbf{F}}_B(\check{k}^+_{B,1})e^{\mathrm{i}\check{k}^+_{B,1}x_1} & \cdots & -\hat{\mathbf{F}}_B(\check{k}^+_{B,d-n})e^{\mathrm{i}\check{k}^+_{B,d-n}x_1} \\ \hat{\mathbf{F}}_B(\check{k}^+_{B,1})e^{\mathrm{i}\check{k}^+_{B,1}x_2} & \cdots & \hat{\mathbf{F}}_B(\check{k}^+_{B,d-n})e^{\mathrm{i}\check{k}^+_{B,d-n}x_2} \\ -\mathrm{i}\check{k}^+_{B,1}\hat{\mathbf{F}}_B(\check{k}^+_{B,1})e^{\mathrm{i}\check{k}^+_{B,1}x_1} & \cdots & -\mathrm{i}\check{k}^+_{B,d-n}\hat{\mathbf{F}}_B(\check{k}^+_{B,d-n})e^{\mathrm{i}\check{k}^+_{B,d-n}x_1} \\ \mathrm{i}\check{k}^+_{B,1}\hat{\mathbf{F}}_B(\check{k}^+_{B,1})e^{\mathrm{i}\check{k}^+_{B,1}x_2} & \cdots & \mathrm{i}\check{k}^+_{B,d-n}\hat{\mathbf{F}}_B(\check{k}^+_{B,d-n})e^{\mathrm{i}\check{k}^+_{B,d-n}x_2} \end{pmatrix}$$

$$\mathbf{Q}_{\hat{b}} = \begin{pmatrix} -\hat{\mathbf{F}}_B(\hat{k}^-_{B,1})e^{\mathrm{i}\hat{k}^-_{B,1}x_1} & \cdots & -\hat{\mathbf{F}}_B(\hat{k}^-_{B,n})e^{\mathrm{i}\hat{k}^-_{B,n}x_1} \\ \hat{\mathbf{F}}_B(\hat{k}^-_{B,1})e^{\mathrm{i}\hat{k}^-_{B,1}x_2} & \cdots & \hat{\mathbf{F}}_B(\hat{k}^-_{B,n})e^{\mathrm{i}\hat{k}^-_{B,n}x_2} \\ -\mathrm{i}\hat{k}^-_{B,1}\hat{\mathbf{F}}_B(\hat{k}^-_{B,1})e^{\mathrm{i}\hat{k}^-_{B,1}x_1} & \cdots & -\mathrm{i}\hat{k}^-_{B,n}\hat{\mathbf{F}}_B(\hat{k}^-_{B,n})e^{\mathrm{i}\hat{k}^-_{B,n}x_1} \\ \mathrm{i}\hat{k}^-_{B,1}\hat{\mathbf{F}}_B(\hat{k}^-_{B,1})e^{\mathrm{i}\hat{k}^-_{B,1}x_2} & \cdots & \mathrm{i}\hat{k}^-_{B,n}\hat{\mathbf{F}}_B(\hat{k}^-_{B,n})e^{\mathrm{i}\hat{k}^-_{B,n}x_2} \end{pmatrix}$$

$$\mathbf{Q}_{\check{b}} = \begin{pmatrix} -\hat{\mathbf{F}}_B(\check{k}^-_{B,1})e^{\mathrm{i}\check{k}^-_{B,1}x_1} & \cdots & -\hat{\mathbf{F}}_B(\check{k}^-_{B,d-n})e^{\mathrm{i}\check{k}^-_{B,d-n}x_1} \\ \hat{\mathbf{F}}_B(\check{k}^-_{B,1})e^{\mathrm{i}\check{k}^-_{B,1}x_2} & \cdots & \hat{\mathbf{F}}_B(\check{k}^-_{B,d-n})e^{\mathrm{i}\check{k}^-_{B,d-n}x_2} \\ -\mathrm{i}\check{k}^-_{B,1}\hat{\mathbf{F}}_B(\check{k}^-_{B,1})e^{\mathrm{i}\check{k}^-_{B,1}x_1} & \cdots & -\mathrm{i}\check{k}^-_{B,d-n}\hat{\mathbf{F}}_B(\check{k}^-_{B,d-n})e^{\mathrm{i}\check{k}^-_{B,d-n}x_1} \\ \mathrm{i}\check{k}^-_{B,1}\hat{\mathbf{F}}_B(\check{k}^-_{B,1})e^{\mathrm{i}\check{k}^-_{B,1}x_2} & \cdots & \mathrm{i}\check{k}^-_{B,d-n}\hat{\mathbf{F}}_B(\check{k}^-_{B,d-n})e^{\mathrm{i}\check{k}^-_{B,d-n}x_2} \end{pmatrix}$$

$$\mathbf{Q}_{\hat{t}} = \begin{pmatrix} \mathbf{0} & \cdots & \mathbf{0} \\ \hat{\mathbf{F}}_A(\hat{k}^+_{A,1})e^{\mathrm{i}\hat{k}^+_{A,1}x_2} & \cdots & \hat{\mathbf{F}}_A(\hat{k}^+_{A,n})e^{\mathrm{i}\hat{k}^+_{A,n}x_2} \\ \mathbf{0} & \cdots & \mathbf{0} \\ \mathrm{i}\hat{k}^+_{A,1}\hat{\mathbf{F}}_A(\hat{k}^+_{A,1})e^{\mathrm{i}\hat{k}^+_{A,1}x_2} & \cdots & \mathrm{i}\hat{k}^+_{A,n}\hat{\mathbf{F}}_A(\hat{k}^+_{A,n})e^{\mathrm{i}\hat{k}^+_{A,n}x_2} \end{pmatrix}$$

$$\mathbf{Q}_{\check{t}} = \begin{pmatrix} \mathbf{0} & \cdots & \mathbf{0} \\ -\hat{\mathbf{F}}_A(\check{k}^+_{A,1})e^{\mathrm{i}\check{k}^+_{A,1}x_2} & \cdots & -\hat{\mathbf{F}}_A(\check{k}^+_{A,d-n})e^{\mathrm{i}\check{k}^+_{A,d-n}x_2} \\ \mathbf{0} & \cdots & \mathbf{0} \\ -\mathrm{i}\check{k}^+_{A,1}\hat{\mathbf{F}}_A(\check{k}^+_{A,1})e^{\mathrm{i}\check{k}^+_{A,1}x_2} & \cdots & -\mathrm{i}\check{k}^+_{A,d-n}\hat{\mathbf{F}}_A(\check{k}^+_{A,d-n})e^{\mathrm{i}\check{k}^+_{A,d-n}x_2} \end{pmatrix}$$

References

[1] X. Antoine, A. Arnold, C. Besse, M. Ehrhardt and A. Schädle, *A Review of Transparent and Artificial Boundary Conditions Techniques for Linear and Nonlinear*

Schrödinger Equations, Commun. Comput. Phys. **4** (2008), 729–796.

[2] A. Arnold, M. Ehrhardt and I. Sofronov, *Discrete Transparent Boundary Conditions for the Schrödinger Equation: Fast calculation, approximation, and stability*, Commun. Math. Sci. **1** (2003), 501–556.

[3] A. Arnold, *Numerically Absorbing Boundary Conditions for Quantum Evolution Equations*, VLSI Design **6** (1998), 313–319.

[4] A. Arnold, *Mathematical concepts of open quantum boundary conditions*, Trans. Theory Stat. Phys. **30** (2001), 561–584.

[5] U. Bandelow, H.-Chr. Kaiser, Th. Koprucki and J. Rehberg, *Spectral properties of* $\mathbf{k}\cdot\mathbf{p}$ *Schrödinger operators in one space dimension*, Numer. Funct. Anal. Optimization **21** (2000), 379–409.

[6] N. Ben Abdallah, P. Degond and P. A. Markowich, *On a one-dimensional Schrödinger-Poisson scattering model*, ZAMP **48** (1997), 135–155.

[7] N. Ben Abdallah and J. Kefi-Ferhane, *Mathematical Analysis of the Two-Band Schrödinger Model* Math. Meth. Appl. Sci. **31** (2008), 1131–1151.

[8] S. Birner, T. Kubis and P. Vogl, *Simulation of quantum cascade lasers - optimizing laser performance*, Photonik International **2** (2008), 60–63.

[9] R. Chen, Z. Xu and L. Sun, *Finite-difference scheme to solve Schrödinger equations*, Phys. Review E **47** (1993), 3799–3802.

[10] M. Ehrhardt, *Discrete Artificial Boundary Conditions*, Ph.D. Thesis, Technische Universität Berlin, 2001.

[11] M. Ehrhardt and A. Arnold, *Discrete transparent boundary conditions for the Schrödinger equation*, Rivista di Matematica della Universit a di Parma **6** (2001), 57-108.

[12] P. Enders and M. Woerner, *Exact* 4×4 *block diagonalization of the eight-band* $\mathbf{k}\cdot\mathbf{p}$ *Hamiltonian matrix for the tetrahedral semiconductors and its application to strained quantum wells*, Semicond. Sci. Technol. **11** (1996), 983–988.

[13] D. Klindworth, *Discrete Transparent Boundary Conditions for Multiband Effective Mass Approximations*, Diploma Thesis, Technische Universität Berlin, 2009.

[14] Th. Koprucki, *Zu* $\mathbf{k}\cdot\mathbf{p}$*-Schrödingeroperatoren*, Ph.D. Thesis, Freie Universität Berlin, 2008.

[15] P. Matus, *Exact difference schemes for time-dependent problems*, Comput. Meth. Appl. Math. **5** (2005), 422–448.

[16] R. E. Mickens, *Difference Equations: Theory and Applications*, Van Nostrand Reinhold, New York, 1990, 2nd ed.

[17] R. E. Mickens, *Novel explicit finite-difference schemes for time–dependent Schrödinger equations*, Comput. Phys. Commun. **63** (1991), 203–208.

[18] R. E. Mickens and I. Ramadhani, *Finite-difference scheme for the numerical solution of the Schrödinger equation*, Phys. Review A **45** (1992), 2074–2075.

[19] R. E. Mickens, *A nonlinear nonstandard finite difference scheme for the linear time-dependent Schrödinger equation*, J. Diff. Eq. Appl. **12** (2006), 313–320.

[20] G. Milovanovic, O. Baumgartner and H. Kosina, *Simulation of Quantum Cascade Lasers using Robin Boundary Conditions*, 9th International Conference on Numerical Simulation of Optoelectronic Devices, Gwangju Institute of Science and Technology, 2009.

[21] C. A. Moyer, *Numerical solution of the stationary state Schrödinger Equation using discrete transparent boundary conditions*, Comput. Sci. Engin. **8** (2006), 32–40.

[22] C. Negulescu, *Numerical analysis of a multiscale finite element scheme for the resolution of the stationary Schrödinger equation*, Numerische Mathematik **108** (2008), 625–652.

[23] A. Ostrowski and H. Schneider, *Some Theorems on the Inertia of General Matrices*, J. Math. Anal. Appl. **4** (1962), 72-84.

[24] R. Pérez-Alvarez and H. Rodriguez-Coppola, *Transfer matrix in 1D Schrödinger problems with constant and position-dependent mass*, Phys. Stat. Sol. (b) **145** (1988), 493–500.

[25] R. Pérez-Alvarez, H. Rodriguez-Coppola V. R. Velasco and F. Garcia-Moliner, *A study of the matching problem using transfer matrices*, J. Phys. C: Solid State Phys. **21** (1988), 2197–2206.

[26] T. E. Simos and P.S. Williams, *On finite difference methods for the solution of the Schrödinger equation*, Computers & Chemistry **23** (1999), 513–554.

[27] U. Wulf, J. Kucera, P. N. Racec and E. Sigmund, *Transport through quantum systems in the R-matrix formalism*, Phys. Rev. **58** (1998), 16209–16220.

[28] A. Zisowsky, *Discrete Transparent Boundary Conditions for Systems of Evolution Equations*, Ph.D. Thesis, Technische Universität Berlin, 2003.

[29] A. Zisowsky, A. Arnold, M. Ehrhardt and Th. Koprucki, *Discrete Transparent Boundary Conditions for transient* $\mathbf{k}\cdot\mathbf{p}$*-Schrödinger Equations with Application to Quantum-Heterostructures*, J. Appl. Math. Mech. (ZAMM) **85** (2005), 793–805.